A localized chimeric hydrogel therapy combats tumor progression through alteration of sphingolipid metabolism

Sanjay Pal,[1,2,a] Nihal Medatwal,[1,3,a] Sandeep Kumar,[1,3,a] Animesh Kar,[1] Varsha Komalla,[1,b] Prabhu Srinivas Yavvari,[4,c] Deepakkumar Mishra,[1] Zaigham Abbas Rizvi,[5] Shiv Nandan,[6] Dipankar Malakar,[7] Manoj Pillai,[7] Amit Awasthi,[5] Prasenjit Das,[8] Ravi Datta Sharma,[6] Aasheesh Srivastava,[4] Sagar Sengupta,[9] Ujjaini Dasgupta,[6,*] and Avinash Bajaj[1,*]

1. Laboratory of Nanotechnology and Chemical Biology, Regional Centre for Biotechnology, NCR Biotech Science Cluster, 3rd Milestone, Faridabad-Gurgaon Expressway, Faridabad-121001, Haryana, India.
2. Kalinga Institute of Industrial Technology, Bhubaneswar-751024, Odisha, India.
3. Manipal Academy of Higher Education, Manipal-576104, Karnataka, India.
4. Department of Chemistry, Indian Institute of Science Education and Research, Bhopal-462066, Madhya Pradesh, India.
5. Translational Health Science and Technology Institute, NCR Biotech Science Cluster, 3rd Milestone, Faridabad-Gurgaon Expressway, Faridabad-121001, Haryana, India.
6. Amity Institute of Integrative Sciences and Health, Amity University Haryana, Panchgaon, Manesar, Gurgaon-122413, Haryana, India.
7. SCIEX, 121 Udyog Vihar, Phase IV, Gurgaon-122015, Haryana, India.
8. Department of Pathology, All India Institute of Medical Sciences, Ansari Nagar, New Delhi-110029, India.
9. National Institute of Immunology, Aruna Asaf Ali Marg, New Delhi-110067, India.

a: authors contributed equally.
b: Current address: University of Technology, Sydney, NSW-2007.
c: Current address: Department of Chemistry and Biochemistry, Freie University, Berlin, Germany.

Corresponding authors:

*Ujjaini Dasgupta, Email: udasgupta@ggn.amity.edu

*Avinash Bajaj, Email: bajaj@rcb.res.in

Table of Contents

1. Supporting Figures

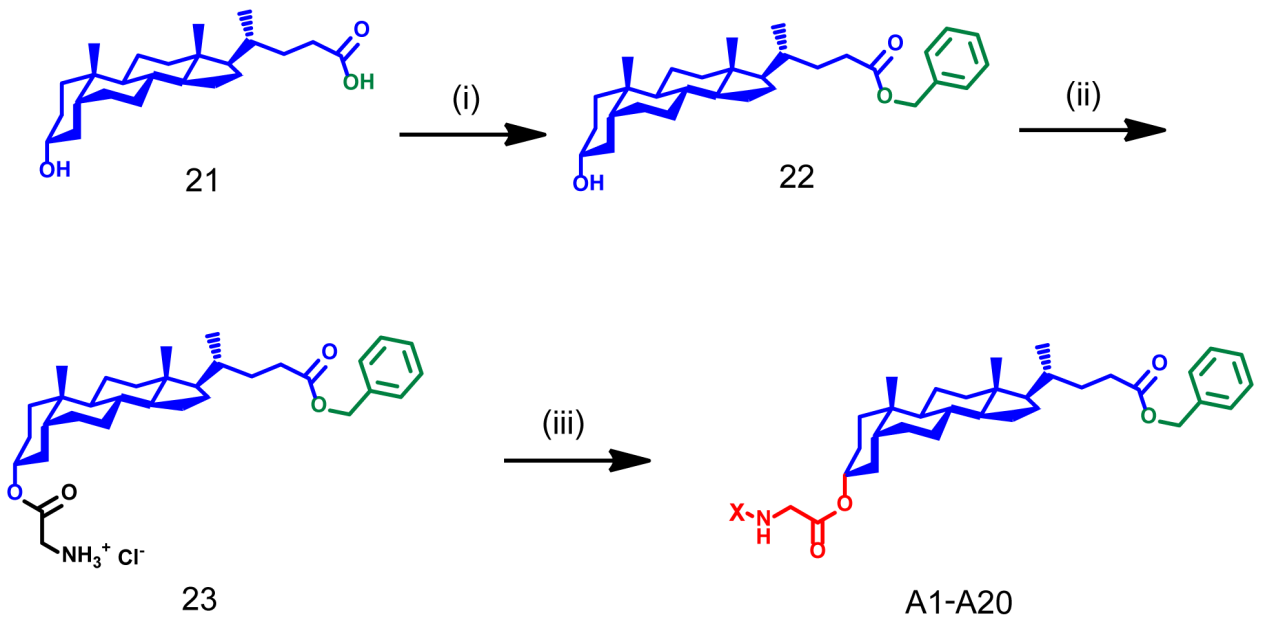

Reagents, reaction conditions and yields: (i) K_2CO_3, Benzyl bromide, DMF, 0 °C - 25 °C, 12 h, 90%. (ii) (a) Boc-Gly-OH, HBTU, DMAP, CH_2Cl_2, 25 °C, 24 h; (b) 4M HCl in Dioxane, 0 °C, 3 h, 95%. (iii) as per experimental section.

Figure S1. Schematic representation showing the synthesis of lithocholic acid (LCA)-dipeptide conjugates where a benzyl group was conjugated to C24-carboxyl terminal of LCA and different dipeptides were appended on 3'-hydroxyl terminals of LCA.

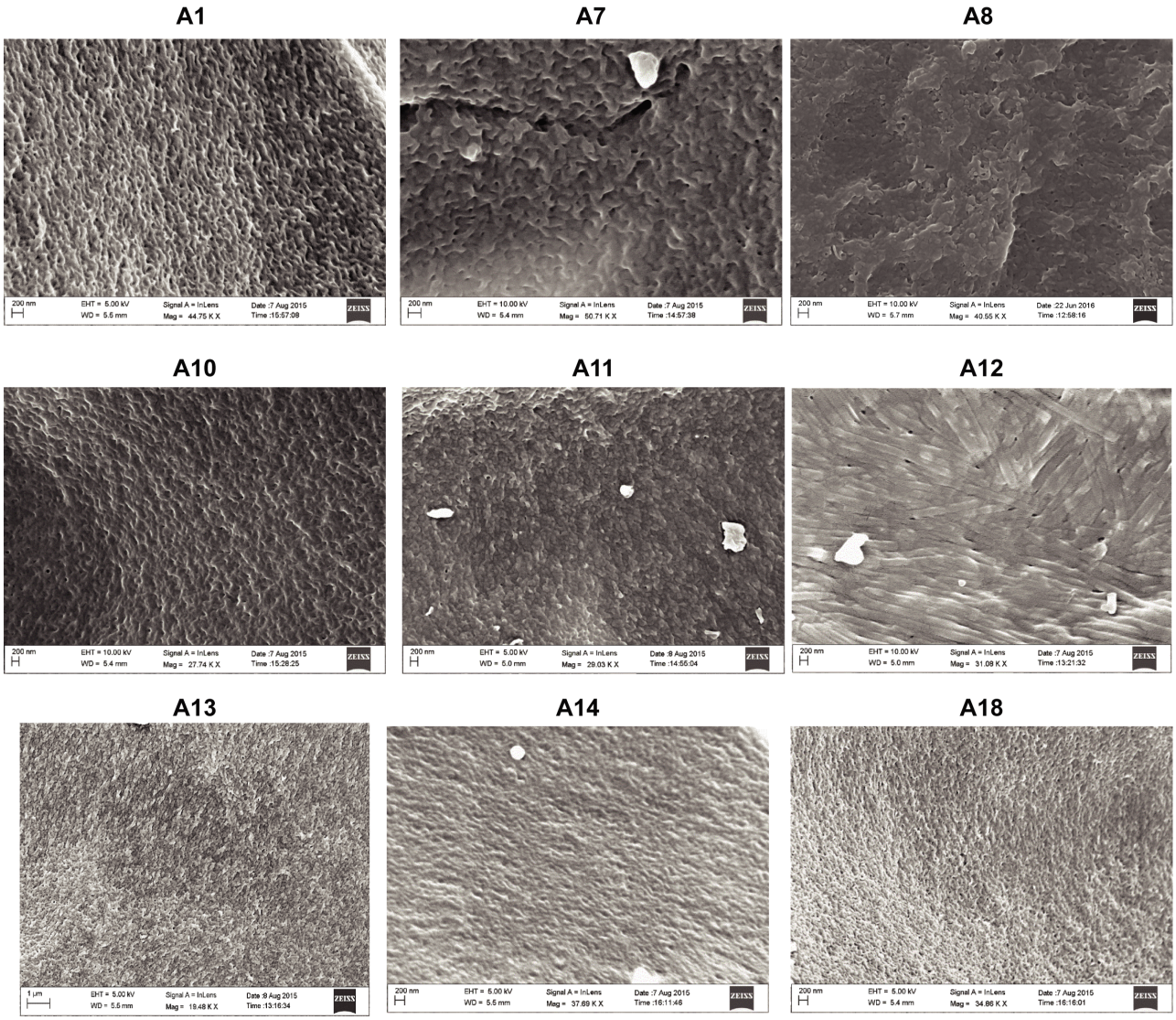

Figure S2. Scanning electron micrographs of hydrogels show highly compact mesh architecture except fibrous architecture for A8 and A12 hydrogels.

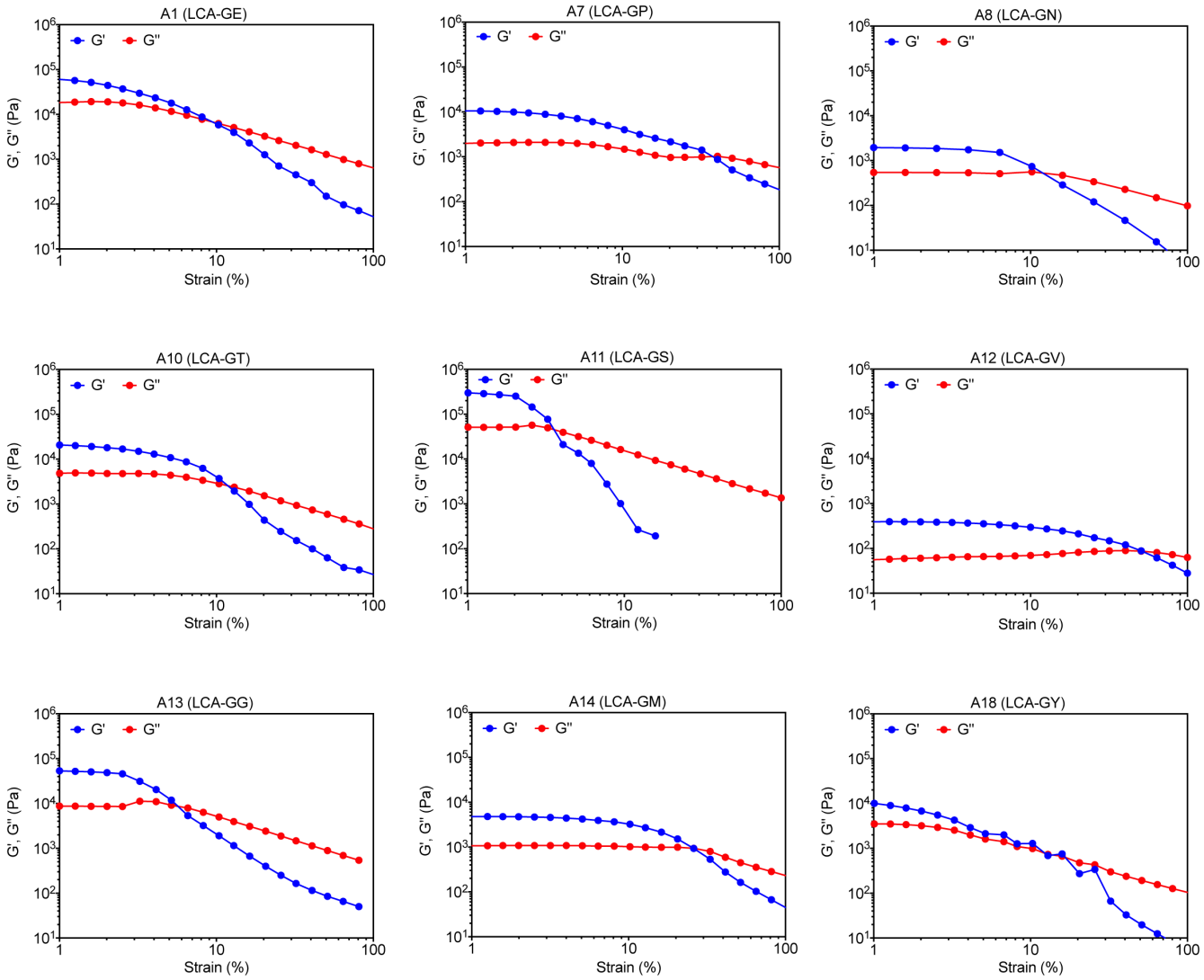

Figure S3. Amplitude sweep profiles of gels under study. Except LCA-GV all hydrogels showed high gel strengths above the order of 10^3.

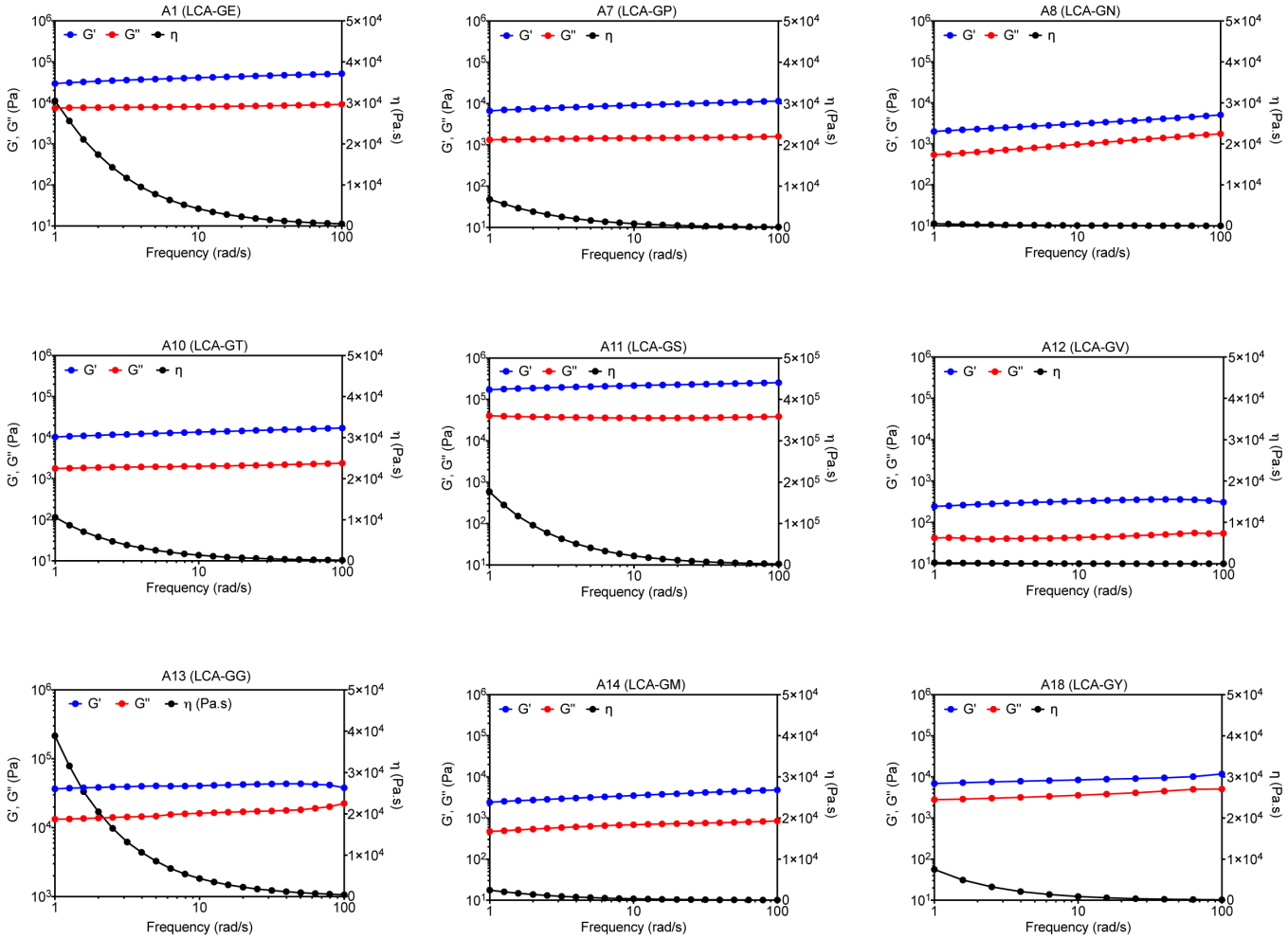

Figure S4. Frequency sweep profiles of gels under study confirming their elastic behavior (with no cross-over points achieved where G' = G") even at a frequency as high as 100 rad s^{-1}.

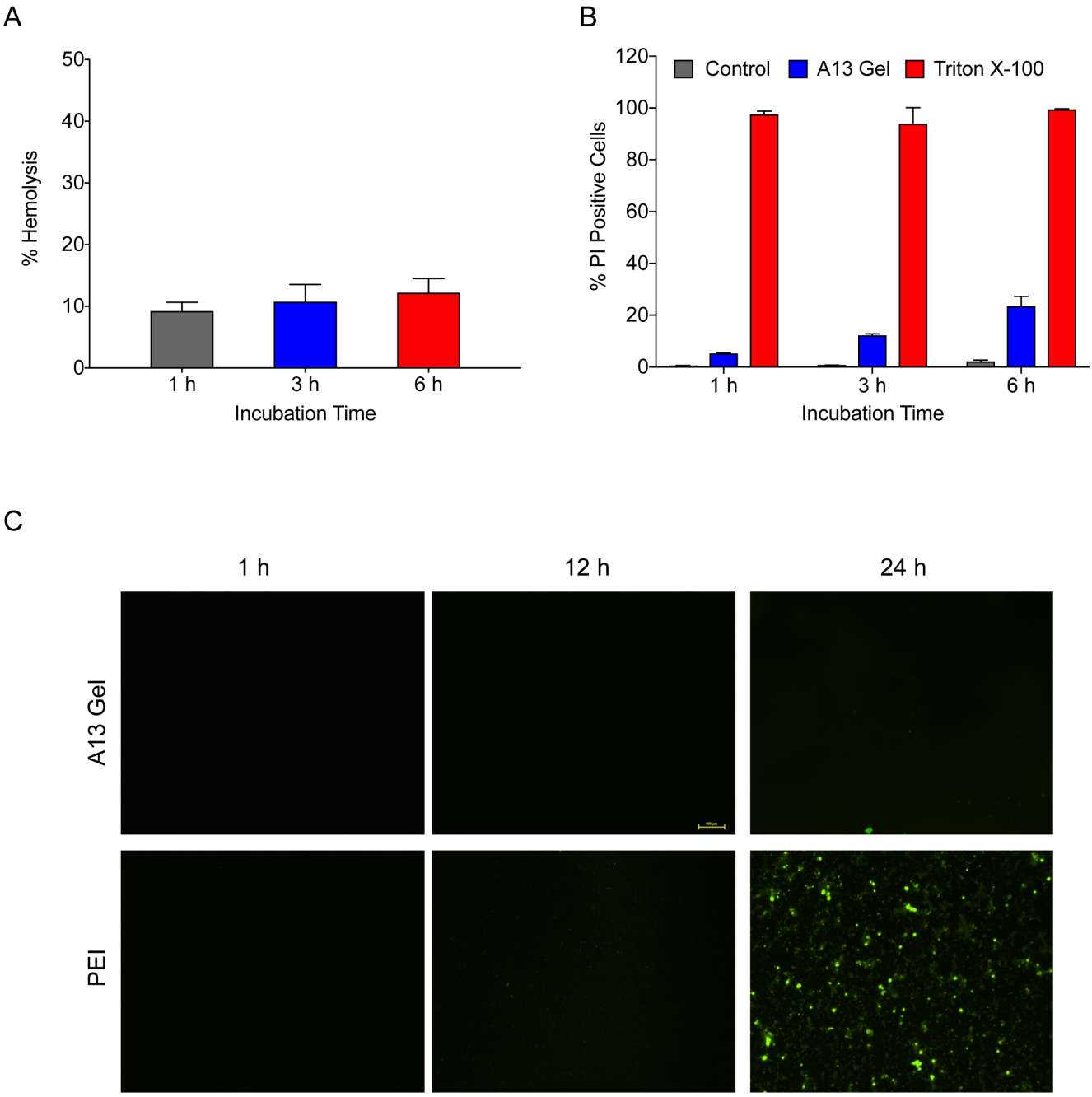

Figure S5. (**A**) Incubation of RBCs with hydrogels for 1, 3 and 6 h confirm only 10% of hemolysis. (**B**) Incubation of peripheral blood mononuclear cells (PBMCs) with hydrogels for 1, 3 and 6 h confirm ~80% cell viability. (**C**) Fluorescence micrographs of A13 gel- and polyethyleneimine (PEI)-coated glass surfaces after incubation with FITC-BSA confirm the inability of BSA to get adsorbed on A13 gel-coated surface.

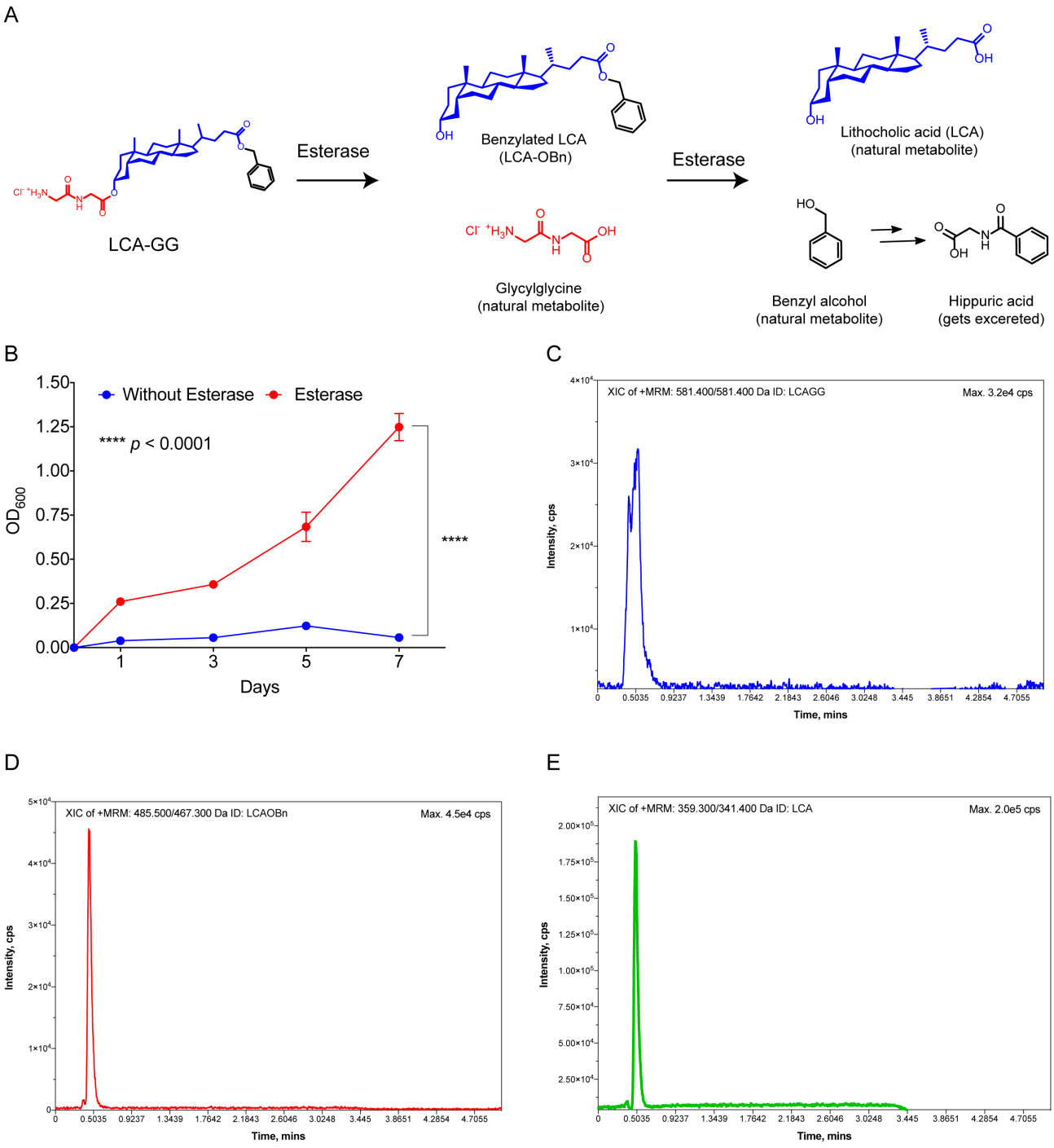

Figure S6. (**A**) Schematic representation showing the possible degradation products of A13 amphiphile by esterase. (**B**) Turbidity assay on incubation of hydrogel with PBS in absence and presence of esterase confirm esterase-mediated increase in turbidity of PBS solution on degradation of the gel. (**C-E**) Extracted-ion chromatogram during Multiple Reaction Monitoring scan confirm the presence of LCA-GG (**C**), LCA-OBn (**D**) and LCA (**E**) in esterase treated samples by LC-MS/MS analysis.

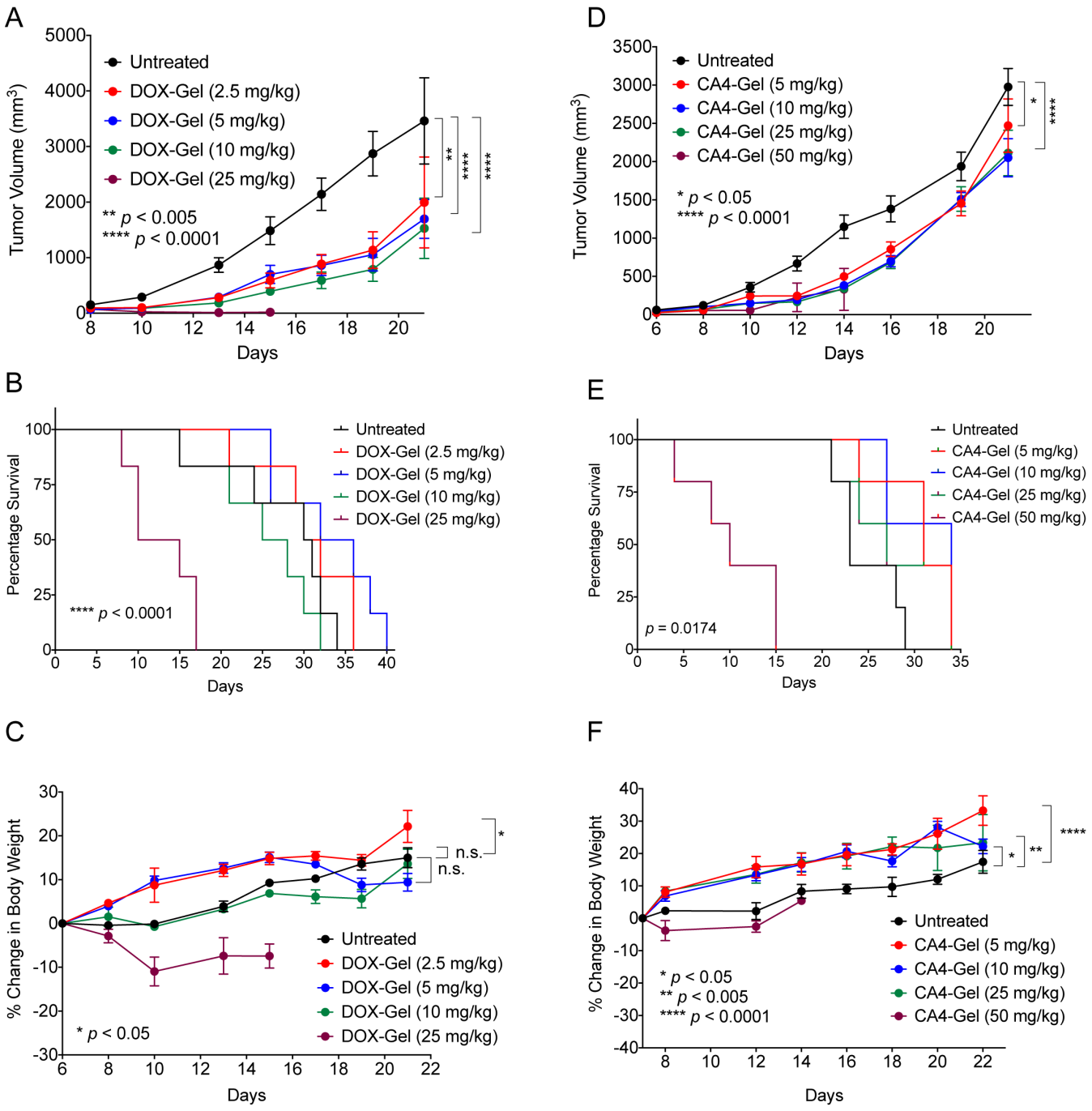

Figure S7. (**A, D**) Tumor growth kinetics (mean ± SEM), (**B, E**) Kaplan-Meier curve (**C, F**) and percentage change in body weight (mean ± SEM) of LLC tumor-bearing mice on treatment with different doses of DOX (**A-C**) or CA4 (**D-F**) entrapped in A13 gel confirm an optimized dose of 5 mg/kg for DOX and CA4. Data was analyzed using two-way ANOVA (**A**, **C, D, F**) and Log-rank Mantel-Cox test (**B, E**).

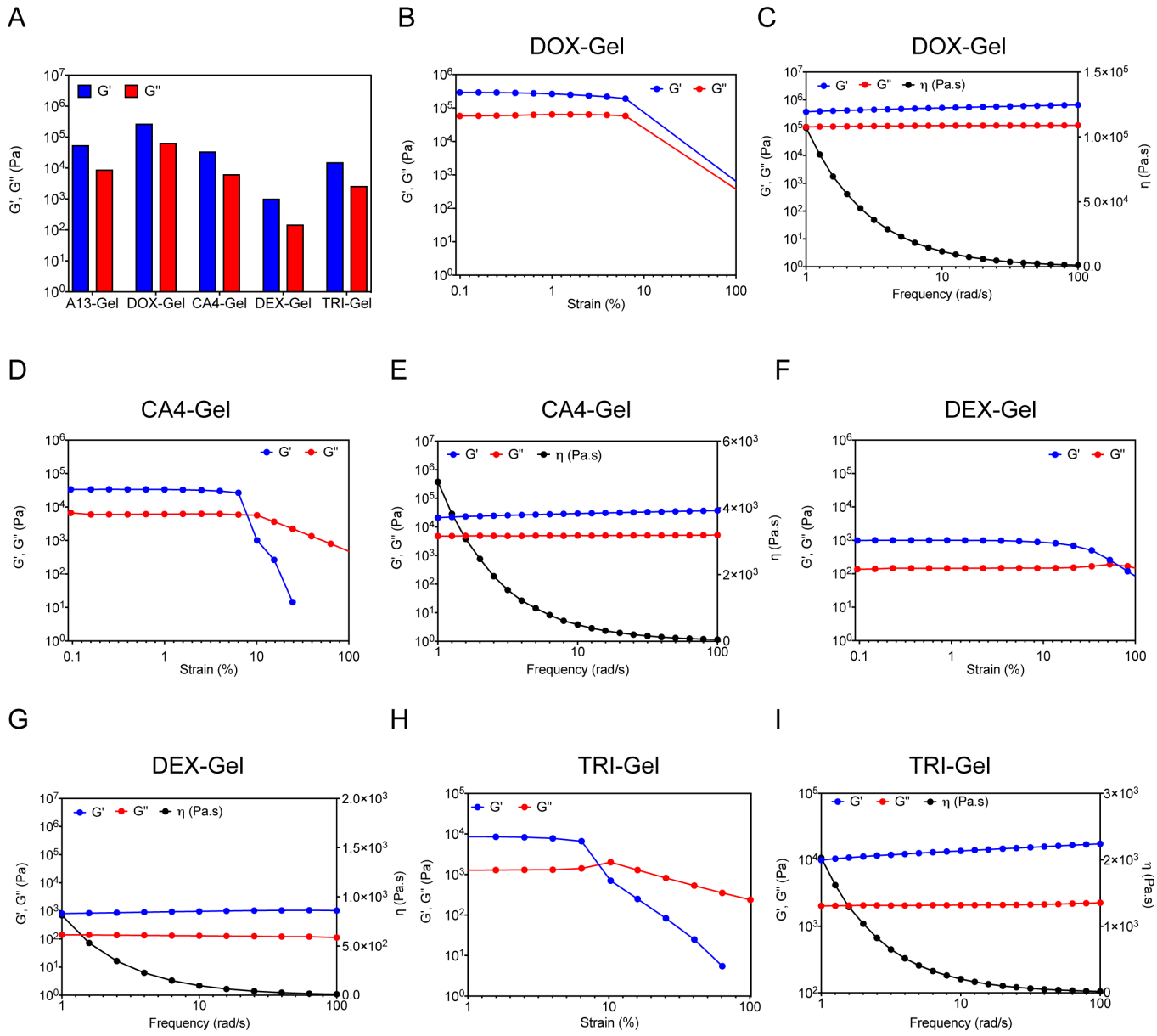

Figure S8. (**A**) Comparison of rheology parameters of A13 gel, DOX-Gel, CA4-Gel, DEX-Gel and TRI-Gel upon entrapment of different drugs in 70 mg of gelator in 1 mL of water. (**B-I**) Amplitude sweep (**B**, **D**, **F, H**) and frequency sweep (**C, E, G, I**) profiles of DOX-Gel (**B**, **C**), CA4-Gel (**D**, **E**) DEX-Gel (**F**, **G**) and TRI-Gel (**H**, **I**) show the ability A13 gel to retain different drugs and combination of drugs.

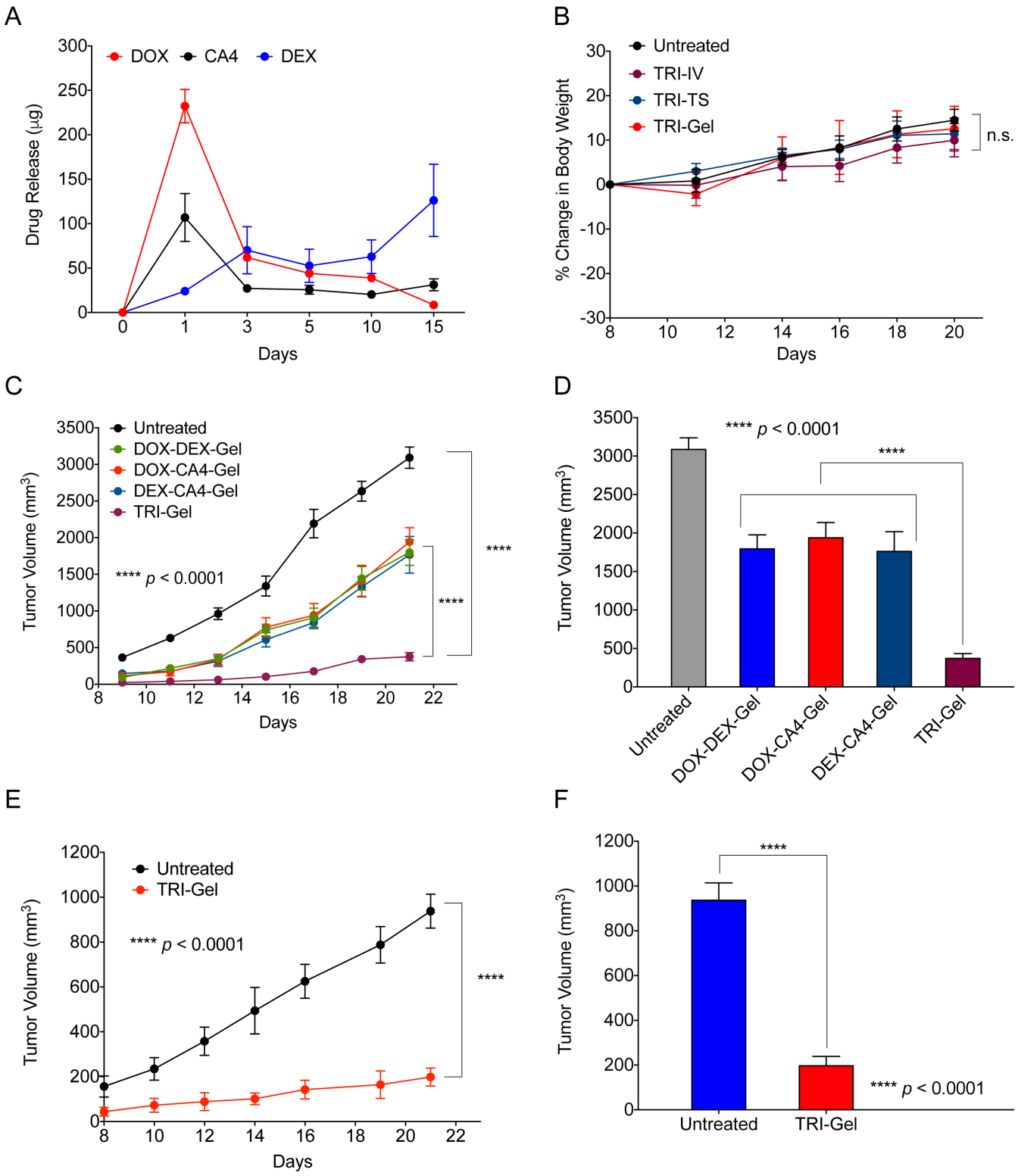

Figure S9. (A) *In vitro* release profiles (mean ± SEM, n = 3) of DOX, CA4 and DEX entrapped in A13 gel (TRI-Gel) showing absolute quantification of drugs. **(B)** Percentage change in body weight (mean ± SEM, n = 7/group) of LLC tumor-bearing mice on TRI-IV, TRI-TS and TRI-Gel treatments confirm no significant decrease in body weight of mice on TRI-Gel treatment. (**C-D**)

Tumor growth kinetics (mean ± SEM, n ≥ 6/group) (**C**) and final tumor volume (mean ± SEM, n ≥ 6/group)) on day 21 (**D**) of LLC tumor-bearing mice on treatment with different combinations of two drugs entrapped in A13 gel and TRI-Gel confirm significant reduction in tumor growth on TRI-Gel therapy as compared to other treatments. **(E-F)** Tumor growth kinetics (mean ± SEM, n = 10/group) (**E**) and final tumor volume on day 21 (**F**) of 4T1-tumor bearing mice on TRI-Gel treatment show significant reduction in tumor growth on TRI-Gel treatment as compared to untreated mice. Data was analyzed using two-way ANOVA (**B, C, E**) and unpaired two-tailed Student's *t*-test (**D, F**).

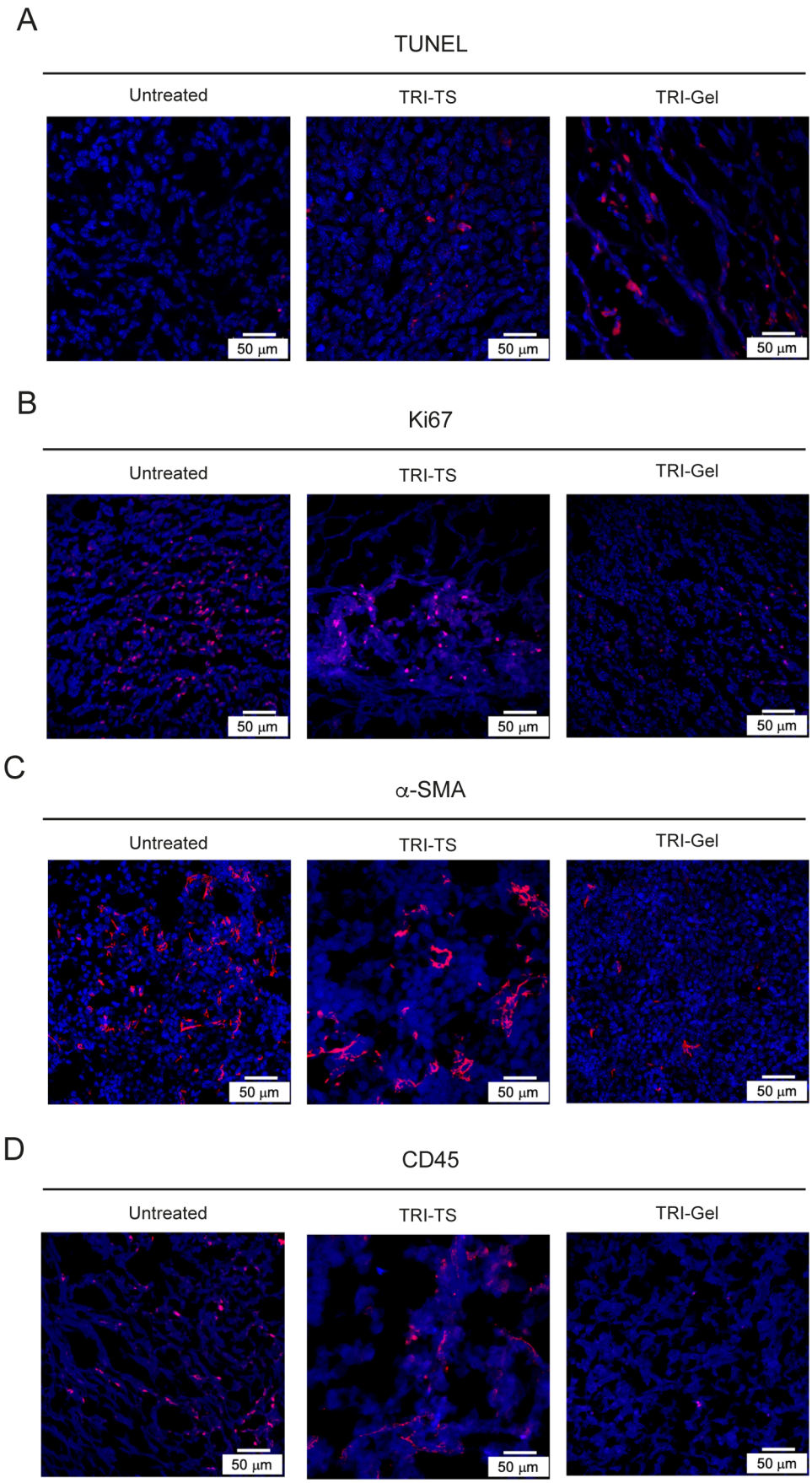
A
TUNEL
Untreated
TRI-TS
TRI-Gel
50 μm
B
Ki67
Untreated
TRI-TS
TRI-Gel
50 μm
C
α-SMA
Untreated
TRI-TS
TRI-Gel
50 μm
D
CD45
Untreated
TRI-TS
TRI-Gel
50 μm

Figure S10. (A-D) Representative fluorescence micrographs of untreated, TRI-TS- and TRI-Gel-treated tumor sections after staining with TUNEL kit (**A**), Ki67 antibody (**B**), α–SMA antibody (**C**) and CD45 antibody confirm significant decrease in proliferation, angiogenesis and inflammation with concurrent increase in apoptosis on TRI-Gel therapy.

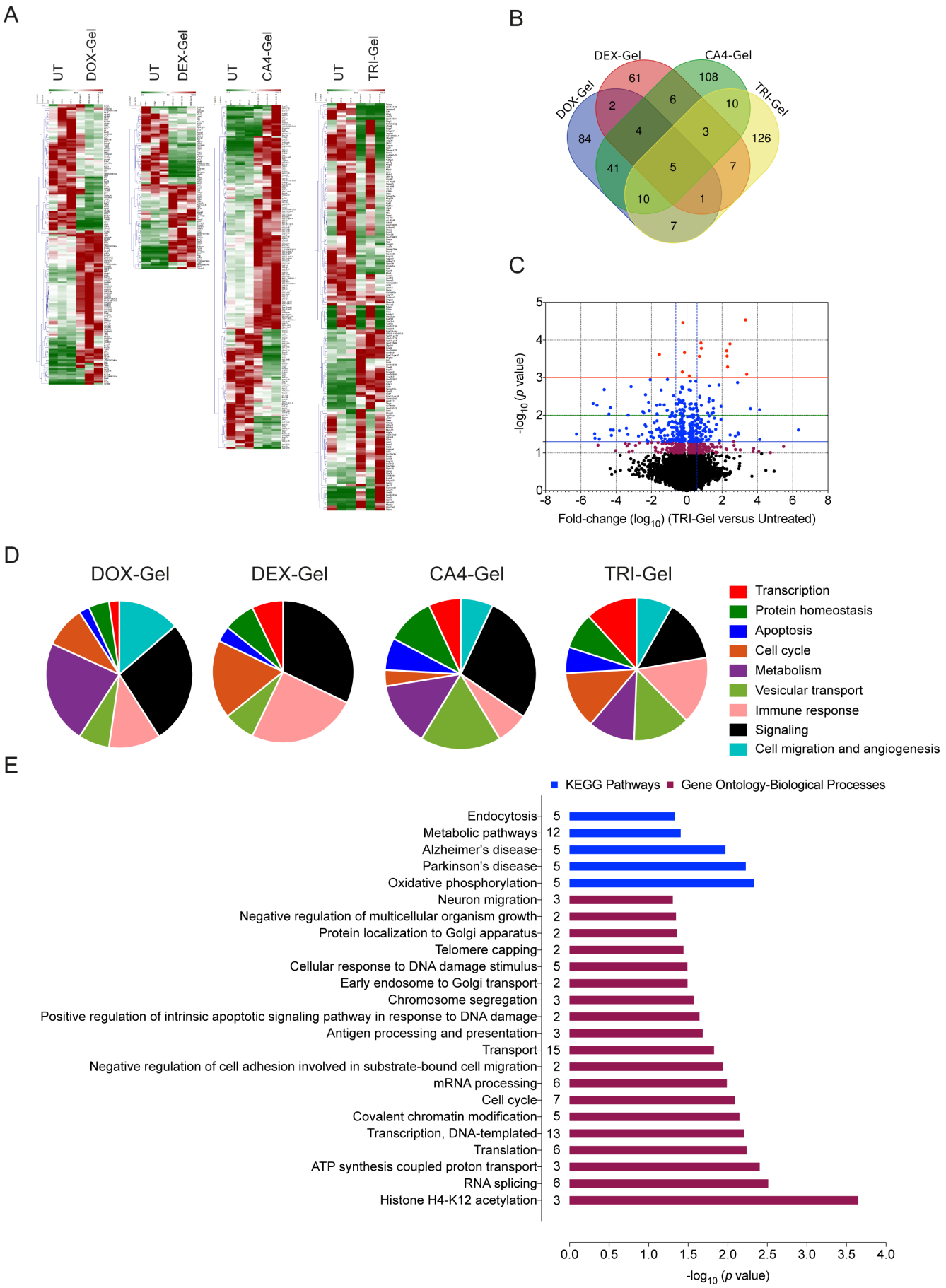
A
UT
DOX-Gel
UT
DEX-Gel
UT
CA4-Gel
UT
TRI-Gel
B
DEX-Gel
CA4-Gel
DOX-Gel
TRI-Gel
61
108
2
6
10
84
4
3
126
41
5
7
10
1
7
C
-log10 (p value)
Fold-change (log10) (TRI-Gel versus Untreated)
D
DOX-Gel
DEX-Gel
CA4-Gel
TRI-Gel
Transcription
Protein homeostasis
Apoptosis
Cell cycle
Metabolism
Vesicular transport
Immune response
Signaling
Cell migration and angiogenesis
E
KEGG Pathways
Gene Ontology-Biological Processes
Endocytosis 5
Metabolic pathways 12
Alzheimer's disease 5
Parkinson's disease 5
Oxidative phosphorylation 5
Neuron migration 3
Negative regulation of multicellular organism growth 2
Protein localization to Golgi apparatus 2
Telomere capping 2
Cellular response to DNA damage stimulus 5
Early endosome to Golgi transport 2
Chromosome segregation 3
Positive regulation of intrinsic apoptotic signaling pathway in response to DNA damage 2
Antigen processing and presentation 3
Transport 15
Negative regulation of cell adhesion involved in substrate-bound cell migration 2
mRNA processing 6
Cell cycle 7
Covalent chromatin modification 5
Transcription, DNA-templated 13
Translation 6
ATP synthesis coupled proton transport 3
RNA splicing 6
Histone H4-K12 acetylation 3
-log10 (p value)

Figure S11. TRI-Gel therapy induces altered and exclusive changes in gene expression.

(**A**) Heat maps showing differential gene expression on transcriptomic analysis of DOX-Gel, DEX-Gel, CA4-Gel and TRI-Gel-treated tumors (n = 3) as compared to untreated (UT) tumors. (**B**) Venn diagram of all differentially expressed genes in LLC tumors in response to DOX-Gel, DEX-Gel, CA4-Gel and TRI-Gel treatments. (**C**) Volcano plot displaying differentially expressed genes in TRI-Gel-treated tumors as compared to untreated (UT) control. (**D**) Ontology analysis of significantly altered genes in response to DOX-Gel, DEX-Gel, CA4-Gel and TRI-Gel treatments show enrichment of genes involved in signaling, immune response, protein homeostasis, transcription, metabolism and cell cycle on TRI-Gel treatment. (**E**) KEGG pathways and Gene-Ontology-Biological Processes predicted by DAVID Functional Annotation tool for differentially expressed genes on TRI-Gel treatment show enrichment of genes involved in vesicular transport, metabolic pathways, translation, mRNA processing, alternative splicing and nuclear export, protein localization to organelles, histone acetylation, chromatin modification, chromosome organization and cell cycle. The number adjacent to each bar represent the genes identified in that category.

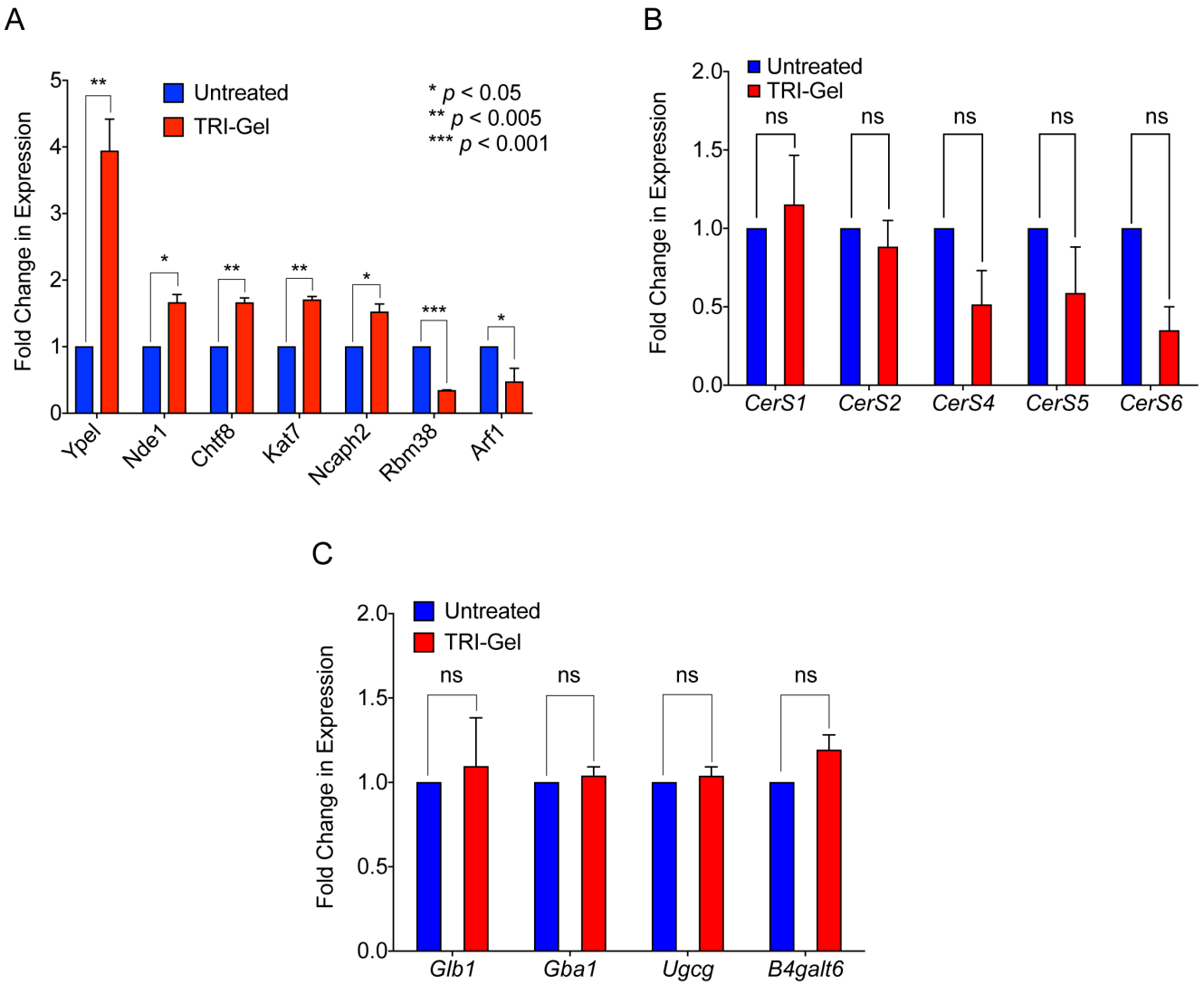

Figure S12. (**A**) qRT-PCR (n = 3) confirm differential expression of selected genes on TRI-Gel treatment as observed in RNA-sequencing data. (**B)** qRT-PCR of ceramide synthases (*Cers1*, *Cers2*, *Cers4*, *Cers5* and *Cers6*) show no significant change in expression on TRI-Gel treatment (n = 3) as compared to untreated tumors (n = 3). (**C**) qRT-PCR of different sphingolipid genes (*Glb1*, *Gba1*, *Ugcg* and *B4galt6*) confirm no significant alteration in their expression on TRI-Gel treatment (n = 3) as compared to untreated tumors (n = 3). Results were analyzed using unpaired two-tailed Student's *t*-test.

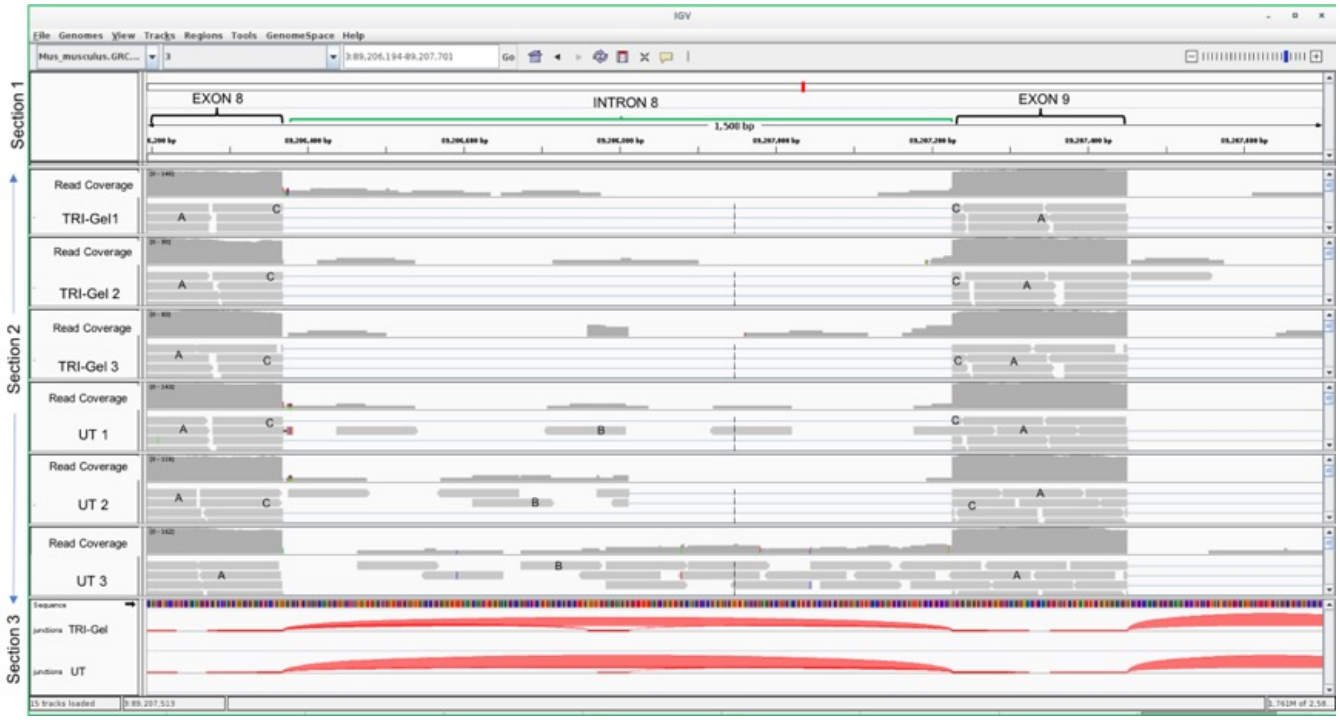

Figure S13. Snapshot taken from IGV software after loading the bam files of samples from TRI-Gel treated (n = 3) and untreated (UT) (n = 3) tumors for intron 8 and its flanking exons (exon 8 and 9) in *Gba1* gene. Section 1 shows corresponding genomic position of exon 8, intron 8 and exon 9 in *Gba1*. Section 2 is divided into 6 rows that correspond to 3 samples of TRI-Gel and UT each. The second column of section 2 shows the reads and coverage of exon 8, intron 8 and exon 9. In this column, reads are marked with flag A, B and C where A shows reads mapped to exon, B shows reads mapped to intron and C shows junction reads. Section 3 shows positions of junctions in 2 samples corresponding to TRI-Gel and UT.

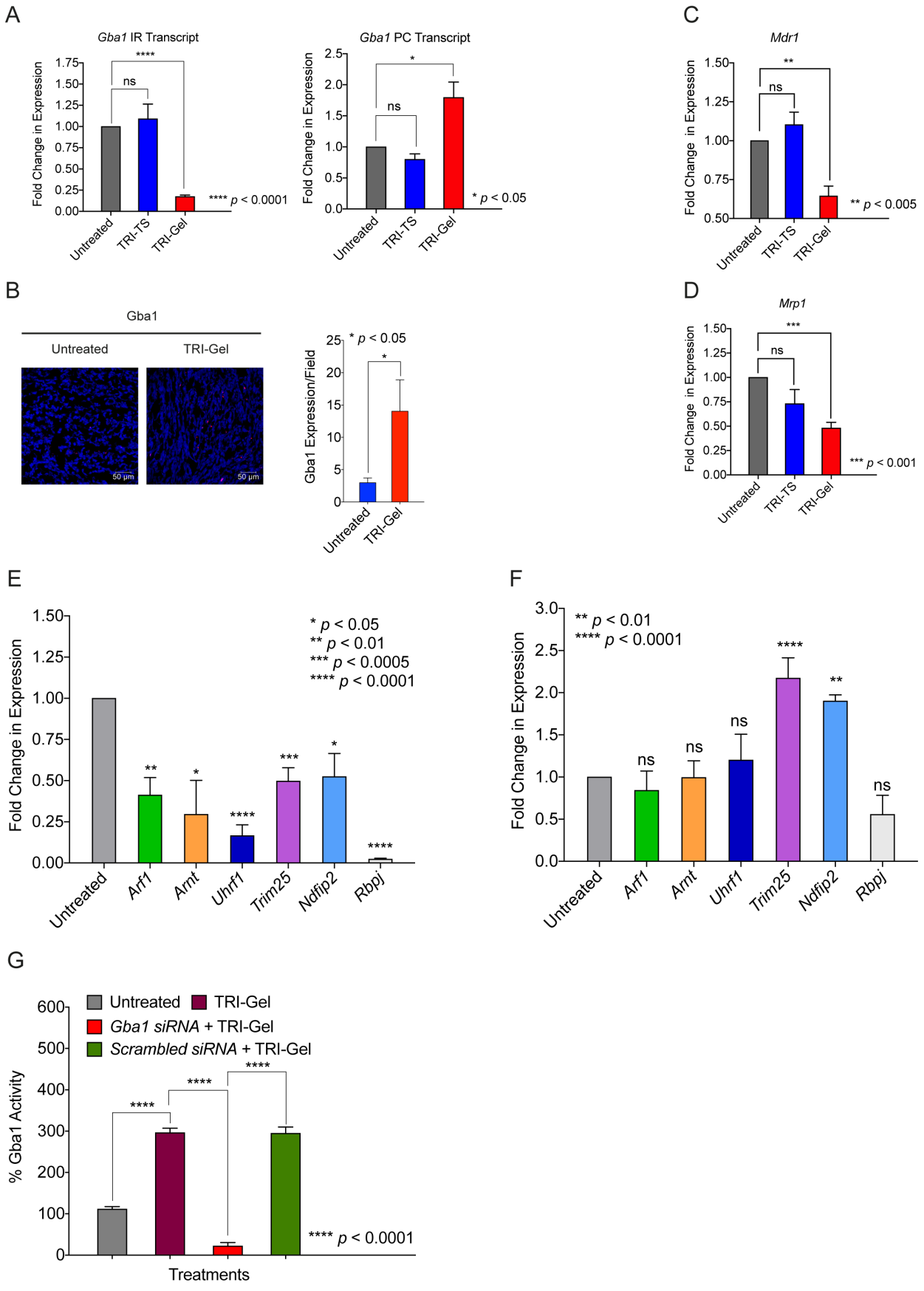
A
Gba1 IR Transcript
Fold Change in Expression
1.75
1.50
1.25
1.00
0.75
0.50
0.25
0.00
****
ns
**** p < 0.0001
Untreated
TRI-TS
TRI-Gel
Gba1 PC Transcript
Fold Change in Expression
2.5
2.0
1.5
1.0
0.5
0.0
*
ns
* p < 0.05
Untreated
TRI-TS
TRI-Gel
C
Mdr1
Fold Change in Expression
1.50
1.25
1.00
0.75
0.50
**
ns
** p < 0.005
Untreated
TRI-TS
TRI-Gel
B
Gba1
Untreated
TRI-Gel
50 µm
50 µm
Gba1 Expression/Field
25
20
15
10
5
0
* p < 0.05
*
Untreated
TRI-Gel
D
Mrp1
Fold Change in Expression
1.50
1.25
1.00
0.75
0.50
0.25
0.00
***
ns
*** p < 0.001
Untreated
TRI-TS
TRI-Gel
E
Fold Change in Expression
1.50
1.25
1.00
0.75
0.50
0.25
0.00
* p < 0.05
** p < 0.01
*** p < 0.0005
**** p < 0.0001
**
*
****
***
*
****
Untreated
Arf1
Arnt
Uhrf1
Trim25
Ndfip2
Rbpj
F
Fold Change in Expression
3.0
2.5
2.0
1.5
1.0
0.5
0.0
** p < 0.01
**** p < 0.0001
ns
ns
ns
****
**
ns
Untreated
Arf1
Arnt
Uhrf1
Trim25
Ndfip2
Rbpj
G
Untreated
TRI-Gel
Gba1 siRNA + TRI-Gel
Scrambled siRNA + TRI-Gel
% Gba1 Activity
600
500
400
300
200
100
0
****
****
****
**** p < 0.0001
Treatments

Figure S14. (**A**) Quantification (mean ± SD, n = 3) of intron retention (IR) and protein coding (PC) transcripts of *Gba1* confirm no significant decrease of IR and increase of PC transcripts on TRI-TS treatment. (**B)** Immunofluorescence images and quantification (mean ± SD, n = 3) of Gba1 in tissue sections reveal >3-fold increase in Gba1 expression on TRI-Gel therapy as compared to untreated tumors. (**C**, **D**) qRT-PCR) of *Mdr1* (**C**) and *Mrp1* (**D**) confirm no significant change in its expression on TRI-TS treatment. (**E-F**) qRT-PCR confirm significant downregulation of *Arf1*, *Arnt*, *Uhrf1*, *Trim25*, *Ndfip2* and *Rbpj* responsible for drug resistance on TRI-Gel (**E**) treatment as compared to untreated tumors whereas TRI-TS treatment (**F**) did not show any significant downregulation of these genes. (**G)** Enzymatic activity (mean ± SEM, n ≥ 5) of Gba1 in tumor tissue lysates on different treatments confirm ~5-fold reduction in Gba1 activity on *Gba1* siRNA + TRI-Gel therapy as compared to TRI-Gel treated mice. Results were analyzed using unpaired two-tailed Student's t-test.

2. Table S1. Table showing gelation properties of amphiphiles in terms of minimum gelation concentration (MGC) and melting temperature (T_m).

Amphiphile	**MGC (mg/mL)**	T_m **(°C)**
A1 (LCA-GE)	60	62
A7 (LCA-GP)	50	59
A8 (LCA-GN	60	65
A10 (LCA-GT)	50	61
A11 (LCA-GS)	50	82
A12 (LCA-GV)	50	61
A13 (LCA-GG)	50	83
A14 (LCA-GM)	50	60
A18 (LCA-GY)	80	62

3. Table S2. List of primers used for validation of differential gene expression.

Gene Name	Forward primer (5' to 3')	Reverse primer (5' to 3')
Arf1	CCAGAACACCCAAGGCTTGATC	AGAACAGCATCTCGGAGCTC
Chtf8	GCTCATCACAGTCCTGCTTCCC	CACCACTGAGGGAATCCCTGTG
Nde1	CAGAGGGCAGAGAATACTCAGG	GCGAAGGCGGTTATTCTCTGAC
Ncaph2	GTATCTGGAGGAGCTGGACC	GCCCTGGATCAACAGTGCTG
Kat7	CCCAAGATTCCAGCCCTGTTCG	GAGCGAGTCTGTCGAAGAGGG
Rbm38	CTACGGCTTCGTGACCATGGC	CCGTCTGTAAGCTCCTAGGC
Uhrf1	GGTCAATGAGTATGTGGACGTGC	CCTCCGAGGTCTTAACGGCAC
Ypel3	CTGTAGTGAATGTGGGCTGCGG	GGTCTTGCAGTTCTCACAGTGG
Gba1	GGCGGTATCTTGGGCATATG	GTAGTAACCCTGTGCCAGTG
Glb1	CGCTGGACATCCTGGTGGAG	CTTGACCCTTGGACCACCCAGG
Ugcg	CCAGAATGATCAGGTGGACC	CAGGCCACAGCATAATCAAG
B4galt6	GTCATCGAACAGACCGGCAC	CAAAGGTCATCGTCCTCGCC
Cers1	CACACATCTTTCGGCCCCTG	CGACAGCCTCCATAGAATCC
Cers2	GGTATGAGAGGCAGAAGGTG	CGTGAATCTCCAGCTGCAAG
Cers4	CTGTGAAGCCTGCTGGAGGT	TCAGCACCAAGGCAGGCTATG
Cers5	CCCTTACTGGAAGCTGCCAAG	CCTGGGTCTAATCCCTCCTG
Cers6	GCTTCCAAGAAAGACTTCGGC	TGTGTGCAGTATCCGTGGAGG
Trim25	CTGGAGAAAGCTGCAAAATTG	CTTCTTAATGGAGTGCTTCAG
Ndfip2	CCTACCACTTCAGATACTGAC	AGACTTACTCTCTGA GGTGC
Rbpj	CATCTTGTCTATTTGACTGCTCC	CTAAAGCAAACTGGTAGCATGAC
Ctnnb1	CAAGTAGCTGATATTGACGG	GCGTCATCCTGATAGTTAATC
Arrb2	GCTAAAGAATAGTGGGGTCT	GAAGTCAGTCTGCTTTTAGC
Csk	CTGTCACCAAGGACCCCAAC	GCTCTGATGCCTTTCCAGGAG
A4galt	GTATAGCCTGCCAGTAGAC	GGTCGTATCCAGACATTAGG
Tcf4	GTTGCCACCAGATGTGCTTC	GATGCTGGAGTATGACTGAATTG
Mdr1	CAAAGAGGCCCTGGATGAAG	CGGAGAATGCTGGCTGTAAG
Mrp1	CATGTGACTCTCAAGGGCTC	CTTCTCACCGATCTCTGTGC
Arnt	CTCACTGATCAGCCCACTTC	GATAAGACTTCTGGAGGGGG
Uhrf1	GGTCAATGAGTATGTGGACGTGC	CCTCCGAGGTCTTAACGGCAC
β-actin	TCTACGAGGGCTATGCTCTCC	GGATGCCACAGGATTCCATAC

4. Table S3. List of primers used for validation of Alternative Splicing events.

Gene/ Oligo Name	Sequence (5'-3')	Position
Topbp1Fa	GGAGGAGCAAAGGTGTTATCTG	Exon-27
Topbp1Ra	GCCGTTTGACTACATTCTCTGC	Exon-28
Topbp1Rb	GACTAGAGAATGGCAGACTGTC	Intron-27-28
Rplp0Fa	GACTGGAGACAAGGTGGGAG	Exon-5
Rplp0Ra	GCCTTGACCTTTTCAFTAAGTG	Exon-6-7 junction
Rplp0Rb	CCACAGGCAGTGTTTTGCTATC	Intron-5-6
Cct3Fa	GTGGGGCACGGATAGTCAGC	Exon-11
Cct3Rb	GTAGACATGCAGCTACAGGCC	Intron-11-12
Cct3Ra	GAACATACACCCGAAGGGAGG	Exon-12-13 junction
G3bp1Fa2	CTTGGGCATCTGTGACGAGTAAG	Exon-8
G3bp1Ra2	CTCACGGATTGGTCGGGGTC	Exon-9-10 junction
G3bp1Rb2	GGAAACACTCCTATCTGCTCC	Intron-8-9
G3bp1	GCTGCGCATCAACAGTGGTG	Exon-11
G3bp1a	GCAGAGGCACCTGAGCCATC	Intron-11-12
G3bp1b	GCCTCTCATCCCACCACTCG	Exon-12
Gba1Fa	CATTTCCCGTGACCTAGGGCC	Exon-8
Gba1Fb	GGTTGCTGGGTCCTACCACC	Intron-8-9
Gba1Ra	GGAGGTTCGTAATGATGCTGTG	Exon-9-10 junction
Dennd6A	CGACAAGTTCGAGATAAAACTC	Exon-5
Dennd6A-1	GCAGGTGGATTTCTGTGAGCAC	Intron-5-6
Dennd6A-2	GCTATCTGTTTGAGTACGGTGTG	Exon-6-7 Junction

5. Legends for Data Figures ES1-ES8 (Figures are in a separate PDF File)

Data Figure ES1. H&E staining of gel and surrounding tissue retrieved after 7, 14 and 21 days of subcutaneous injection of A13 gel and control skin tissues from mice show infiltration of immune cells on day 7 that gets cleared by day 14 and 21, thereby validating biocompatible nature of gel. SC: Stromal cells, FC: Fat cells. Arrow indicates leukocytes. All images were taken at 400X magnification.

Data Figure ES2. CD45 staining of gel and surrounding tissue retrieved after 7, 14 and 21 days of subcutaneous injection of A13 gel and control skin tissues from mice show infiltration of immune cells on day 7 that gets cleared by day 14 and 21, thereby validating biocompatible nature of gel. SC: Stromal cells, FC: Fat cells. Arrow indicates leukocytes. All images were taken at 400X magnification.

Data Figure ES3. Heat map showing differential gene expression on transcriptomic analysis of DOX-Gel treated tumors as compared to untreated (UT) tumors.

Data Figure ES4. Heat map showing differential gene expression on transcriptomic analysis of DEX-Gel treated tumors as compared to untreated (UT) tumors.

Data Figure ES5. Heat map showing differential gene expression on transcriptomic analysis of CA4-Gel treated tumors as compared to untreated (UT) tumors.

Data Figure ES6. Heat map showing differential gene expression on transcriptomic analysis of TRI-Gel treated tumors as compared to untreated (UT) tumors.

Data Figure ES7. Original gel pictures of Figure 4E showing validation of Alternative Splicing by semi-quantitative PCR.

Data Figure ES8. Original gel pictures of Figure 5B showing validation of removal of intron 8 retention event in *Gba1* and of and Figure 5E showing original immunoblot of Gba1.

6. Legends for data sets 1-9 (Data sets are in separate excel files)

Data set 1. Different sphingolipid species with corresponding precursor ion Q1 and product ion Q3, and peak area from 4 biological and 3 technical replicates and fold change of respective sphingolipids for TRI-Gel treated tumor over untreated samples.

Data set 2. Differentially expressed genes after DOX-Gel, DEX-Gel, CA4-Gel, and TRI-Gel treatments as compared to untreated control. Significantly upregulated (p value ≤ 0.05 and fold change (≥1.5) are marked in pink and significantly downregulated genes (p value ≤ 0.05 and fold change (≤ 1.5) are marked in green.

Data set 3. Functions of differentially expressed genes by Gene Ontology (GO) analysis and KEGG pathways on DOX-Gel, DEX-Gel, CA4-Gel, and TRI-Gel treatments. All terms and pathways shown in the corresponding figures have p value ≤ 0.05, Fisher Exact test.

Data set 4. Ontology (GO) analysis of differentially expressed genes on DOX-Gel, DEX-Gel, CA4-Gel and TRI-Gel treatments that are categorized into nine key biological processes.

Data set 5. Cassette Exon events predicted after DOX-Gel, DEX-Gel, CA4-Gel and TRI-Gel treatments.

Data set 6. Intron Retention events predicted after DOX-Gel, DEX-Gel, CA4-Gel and TRI-Gel treatments.

Data set 7. Different Biological Processes (BP) and KEGG pathways enriched for Cassette Exon (CE) events observed on DOX-Gel, DEX-Gel, CA4-Gel and TRI-Gel treatments.

Data set 8. Different Biological Processes (BP) and KEGG pathways enriched for different Intron Retention (IR) events observed on DOX-Gel, DEX-Gel, CA4-Gel and TRI-Gel treatments. All terms and pathways shown in Figure 4D have p value ≤ 0.05, Fisher's Exact test and FDR ≤ 25.0.

Data set 9. Cassette exon and intron retention events in sphingolipid genes on DOX-Gel, DEX-Gel, CA4-Gel and TRI-Gel treatments.

7. Materials

REAGENT	SOURCE	IDENTIFIER
Chemicals and solvents used for synthesis		
Lithocholic acid	Sigma	Cat# L469180; CAS Number 434-13-9
Benzyl bromide	Sigma	Cat# B17905; CAS Number 100-39-0
Potassium carbonate	Sigma	Car# 791776; CAS Number 584-08-7
Dichloromethane	Sigma	Cat# 270997; CAS Number 75-09-2
N,*N*-Dimethyl formamide	Sigma	Cat# 227056; CAS Number 75-12-7
HBTU	Sigma	Cat# 12804; CAS Number 94790-37-1
4-(Dimethylamino)pyridine	Spectrochem	Cat# 1004194; CAS Number 1122-58-3
Hydrochloric acid (4M) in Dioxane	Spectrochem	Cat# 0108141; CAS Number 172611-77-7
Diethyl ether	S D Fine-Chem	Cat# 20912; CAS Number 60-29-7
N,N-ethylcarbodiimide Hydrochloride (EDC)	Sigma	Cat# 03450; CAS Number 25952-53-8
1-Hydroxybenzotriazole monohydrate (HOBT)	HiMedia Labs	Cat# RM9617; CAS Number 123333-53-9
N,*N*-Diisopropylethylamine (DIPEA)	Sigma	Cat# 550043; CAS Number 7087-68-5
Trifluoroacetic acid (TFA)	S D Fine-Chem	Cat# 40508; CAS Number 76-05-1
Amberlite IRA-900 chloride	Sigma Aldrich	Cat# 216585; CAS Number 9050-97-9
Silica gel 230-400 mesh	Merck Millipore	Cat# 109385; CAS Number 7631-86-9
Petroleum ether	Thermo Fisher	Cat# E139-20; CAS Number 101316-46-5
Ethyl acetate (EtOAc)	Thermo Fisher	Cat# E145-20; CAS Number 141-78-6
Dichloromethane (DCM)	Finar	Cat# 10550LL025; CAS Number 75-09-2
Methanol (MeOH)	Finar	Cat# 10930LL025; CAS Number 67-56-1
Boc-Glycine	Spectrochem	Cat# 0102184; CAS Number 4530-20-5
Boc-Leu-OH	Fluka	Cat# 15450; CAS Number 13139-15-6
Boc-Arg(Pbf)-OH	Sigma	Cat# 15038; CAS Number 200124-22-7
Boc-Asn(Trt)-OH	Nova Biochem	Cat# 853074; CAS Number 132388-68-2
Boc-Asp-OtBu	Sigma	Cat# 742325; CAS Number 34582-32-6
Boc-Cys(Trt)-OH	Sigma	Cat# 459313; CAS Number 21947-98-8
Boc-Gln(Trt)-OH	Sigma	Cat# 5563; CAS Number 132388-69-3

Boc-His(Boc)-OH.DCHA	Nova Biochem	Cat# 8.53067; CAS Number 31687-58-8
Boc-Glu(OtBu)-OH	Sigma	Cat# 15436; CAS Number 24277-39-2
Boc-Val-OH	Sigma	Cat# 15528; CAS Number 13734-41-3
Boc-L-Lys(BOC)-OH.DCHA	Sisco Research	Cat# 0248304; CAS Number 15098-69-8
Boc-Methionine	Sisco Research	Cat# 0248344; CAS Number 2488-15-5
Boc-Phenylalanine	Sisco Research	Cat# 0248222; CAS Number 13734-34-4
Boc-Proline	Sisco Research	Cat# 0248224; CAS Number 15761-39-4
Boc-Serine	Sisco Research	Cat# 0248226; CAS Number 3262-72-4
Boc-Threonine	Sisco Research	Cat# 0248228; CAS Number 2592-18-9
Boc-Tryptophan	Sisco Research	Cat# 0248230; CAS Number 13139-14-5
Boc-Tyrosine	Sisco Research	Cat# 0248231; CAS Number 3978-80-1
Boc-Isoleucine	Sisco Research	Cat# 0248217; CAS Number 13139-16-7
Boc-Alanine	Sisco Research	Cat# 0248204; CAS Number 15761-38-3

Chemicals for lipidomics studies

Methanol (MS Grade)	Honeywell	Car# 34966; CAS Number 67-56-1
Chloroform (MS Grade)	Honeywell	Car# 25669-1L; CAS Number 67-66-3
Formic acid (MS Grade)	Fluka	Car# 56302-50ML; CAS Number 64-18-6
Ammonium formate	Fluka	Cat# 14266-25G; CAS Number 540-69-2
Acetonitrile	Honeywell	Car# 34967
Ammonium acetate	Honeywell	Cat#14267-25G
Ammonium hydroxide	ThermoFisher	Cat#16227, CAS Number 1336-21-6
Water (MS Grade)	Riedel-de haen	Cat# 39253-4L; CAS Number 7732-18-5
Potassium hydroxide	Sisco Research	Cat# 84749; CAS Number 1310-58-3
Glacial acetic acid	Merck	Cat# 193402
ACQUITY UPLC BEH Shield RP18 column	Water Ltd.	Cat# 186002854
Cer/SPh mixture II	Avanti Polar Lipids	Cat# LM6005
Sphingolipid standards	Avanti Polar Lipids	Cat# 860516P, 860539P, 860533P, 860576P, 860492P

Biochemicals and kits

Collagenase	Sigma	Cat# C5138
DNase I	Sigma-Aldrich	Cat# D4527

Annexin-FITC assay kit	BioLegend	Cat# 640906
Esterase	Sigma-Aldrich	Cat# E3019-20KU
RNAiso Plus	DSS Takara	Cat# 9109
Ethanol	Merck	Cat# 100983; CAS Number 64-17-5
MOPS, free acid	Bio basic	Cat# MB0360
Formaldehyde	HiMedia	Cat# MB059; CAS Number 50-00-0
Ethidium bromide	Sigma	Cat# E8751; CAS Number 1239-45-8
100 bp DNA ladder	BR Biochem	Cat# BM001-R500
DNase I, RNase-free	Thermo Fisher	Cat# EN0521
iScript™ cDNA synthesis kit	Bio-Rad	Cat# 1708891
Promega™ GoTaq™ Flexi DNA polymerase	Promega	Cat# PR-M8295
Deoxynucleotide (dNTP) Solution mix	New England Biolabs	Cat# N0447S
Agarose	Sigma	Cat# A9539; CAS Number 9012-36-6
iTaq™ universal SYBR®Green supermix	Bio-Rad	Cat# 1725124
Ethylenediaminetetraacetic acid disodium salt dihydrate	Sigma	Cat# E5134; CAS Number 6381-92-6
Xylene cyanol FF	Sigma	X4126; CAS Number 2650-17-1
Hydrochloric acid	Thermo Fisher	Cat# 29505; CAS Number 7647-01-0
Bromophenol blue sodium salt	Sigma	Cat# B8026; CAS Number 34725-61-6
Sodium dodecyl sulfate	Sigma	Cat# L3771; CAS Number 151-21-3
Acrylamide	Bio basic	Cat# AB1032; CAS Number 79-06-1
Polyoxyethylenesorbitan monolaurate (Tween® 80)	HiMedia	Cat# GRM156; CAS Number 9005-64-5
Polyoxyethylenesorbitan monolaurate (Tween® 20)	HiMedia	Cat# P7949; CAS Number 9005-64-5
Glycerol	HiMedia	Cat# GRM1027; CAS Number 56-81-5
Ammonium persulfate	Sigma	Cat# A3678; CAS Number 7727-54-0

Phenylmethanesulfonyl fluoride	Sigma	Cat# P7626; CAS Number 329-98-6
N,*N*′-methylenebisacrylamide	Sigma	Cat# M7279; CAS Number 110-26-9
Sodium chloride	HiMedia	Cat# GRM853; CAS Number 7647-14-5
Glycine	Sigma	Cat# G8898; CAS Number 56-40-6
Bovine serum albumin fraction-V	HiMedia	Cat# GRM105; CAS Number 9048-46-8
Chemiluminescent HRP substrate	Merck	Cat# WBKLS0500
Pierce™ BCA protein assay kit	ThermoScientific	Cat# 23227
Hoechst 33258	Sigma	Car# 861405; CAS Number 23491-45-4
Paraformaldehyde	Thomas baker	Cat# 81847; CAS Number 50-00-0
Cryomatrix	Thermo Scientific	Cat# 6769006
Poly-lysine slides	Sigma	Cat# P0425
Goat serum	HiMedia	Car# RM10701
Allprotect Tissue Reagent	Qiagen	Cat# 76405
Cryomatrix	ThermoFisher scientific	Cat# 6769006
Mice bleeding cap	Top tech lab	Cat# T10H09
Peel-A-Way embedding molds	Sigma	Cat# E6032
IR-820	Sigma	Cat# 543365; CAS Number 172616-80-7
In Situ Cell Death Detection Kit	Roche	Cat# 12156792910
Prolong gold anti-fade reagent	Life technologies	Cat# P36934
Sectioning blade	Microm	Cat# 152580
Triton X-100	Sigma	Cat# T9284; CAS Number 9002-93-1
Taurocholic acid sodium	Sigma	Cat# T4009; CAS Number 345909-26-4
BSA	Bio-Rad	Cat# 500-0206

4-methylumbelliferyl β-glucopyranoside	Sigma	Cat# M3633; CAS Number 18997-57-4
4-methylumbelliferone	Sigma	Car# M1381; CAS Number 90-33-5
Citric acid	Sigma	Cat# 251275; CAS Number 77-92-9
Disodium hydrogen orthophosphate dihydrate	S D Fine	Cat# 40158; CAS Number 7558-79-4
Sodium hydroxide	S D Fine	Cat# 40167; CAS Number 1310-73-2
Developer	Carestream	Cat# 4908216
XBT X-Ray film	Carestream	Cat# 6568307
Mayer's Hematoxylin	Sigma	Cat# MHS16
Eosin Y solution	Sigma	Cat# HT110316
Lithium carbonate	Merck	Cat# ME9M581310; CAS Number 554-13-2
Xylene	Thomas Baker	Cat# 167214; CAS Number 1330-20-7
DPX mounting medium	Sigma	Cat# 06522
DAB enhanced liquid substrate	Sigma	Cat# D3939
Antibodies		
CD45-APC-Cy 7	BioLegend	Cat# 103115
CD31-APC	BioLegend	Cat# 102409
Ki67-PerCp	BioLegend	Cat# 652423
Zombie Violet™ Fixable Viability Kit (BV421™)	BioLegend	Cat# 423113
Anti-Ki67 for IHC	BioLegend	Cat# 652402, RRID:AB_11204254
Anti-CD45 for IHC	BioLegend	Cat# 103102, RRID:AB_312967
Anti-P-glycoprotein	Abcam	Cat# AB170904, RRID:AB_2687930
Anti-actin, α-smooth muscle	Sigma	Cat# A2547, RRID:AB_476701
Anti-β-glucocerebrosidase 1	Abcam	Cat# AB175869
Secondary IgG anti-mouse-Alexa fluor 594	Cell Signaling	Cat# 88903

Secondary IgG anti-rabbit-Alexa fluor 594	Cell Signaling	Cat# 88893
Anti-β-actin	Sigma	Cat#A5441, RRID:AB_476744
Secondary anti-mouse HRP conjugated IgG Antibody	Thermo Fisher	Cat# 61-6520, RRID:AB_2533933
Cell culture reagents		
Antibiotic solution (100X)	HiMedia	Cat# A001A
DMEM media	Sigma	Cat# D5648
DPBS	Sigma	Cat# D5652
FBS	Gibco	Cat# 10270
Matrigel matrix	Corning	Cat# 354234
Plasmocin prophylactic	InvivoGen	Cat# ANT-MPP
Plasmocin treatment	InvivoGen	Cat# ANT-MPT
Trypsin	HiMedia	Cat# TCL007
Oligonucleotides		
Gba1 siRNA	Dharmacon	L-057341-01-0005
Scrambled siRNA	Dharmacon	D-001630-01
Primers for AS validation	This Paper	Table S2
Primers for Real- Time PCR	This Paper	Table S3

8. Methods

8.1. Safety statement. All the experiments presented in this manuscript are generally safe and no unexpected or unusual high safety hazards were encountered.

8.2. Synthesis and characterization of amphiphiles (Figure S1). All the amphiphiles were synthesized as mentioned below. ^{1}H NMR spectra were recorded in DMSO-d_6, Methanol-d_4, D_2O and $CDCl_3$ using a Bruker Avance 400 MHz spectrometer. Chemical shifts (δ) are reported in ppm with tetramethylsilane (TMS) as the internal standard. Mass spectrometry analysis was performed with Bruker micrOTOF-Q II 10330.

Synthesis of compound **22**. Lithocholic acid (**21**) (5 g, 1 equiv) was taken in anhydrous dimethylformamide (20 mL) in a round bottom flask with a magnetic bead. Potassium carbonate (2 equiv) was added to the solution followed by drop wise addition of benzyl bromide (1.2 equiv) at 0 ºC. The reaction mixture was allowed to stir at 25 ºC for 12 h. The reaction mixture was then diluted with ethyl acetate (200 mL) and washed with saturated $NaHCO_3$ solution (2 x 100 mL) and 2N HCl (2 x 100 mL). The organic layer was separated and dried over anhydrous Na_2SO_4. The solvents were evaporated under reduced pressure and the crude product was purified by silica gel (230-400 mesh) combi-flash column chromatography using ethyl acetate – petroleum ether (20 %) as eluents to obtain a white solid **22**. Yield: 90%. ^{1}H-NMR (400 MHz, $CDCl_3$): *δ* 0.61 (s, 3H), 0.89-1.95 (m, steroid), 2.25-2.39 (m, 2H), 3.61-3.62 (m, 1H), 5.08-5.14 (m, 2H), 7.25-7.36 (m, 5H).

Synthesis of compound **23**. (a) Compound (**22**) (2.0 g, 1 equiv), DMAP (0.3 equiv), and Boc-Gly-OH (1.5 equiv) were dissolved in dry dichloromethane (15 mL) and stirred at 0 °C for 15 min. HBTU (1.5 equiv) was added to the reaction mixture portion wise and the reaction was allowed to stir for 24 h at 25 ºC. The crude mixture was diluted with ethyl acetate (200 mL), and washed with saturated $NaHCO_3$ (2 x 100 mL) and brine (2 x 100 mL) solution. The organic layer was separated and dried over anhydrous Na_2SO_4. Solvents were evaporated under reduced pressure and the crude product was purified by silica gel (230-400 mesh) column chromatography using ethyl

acetate – petroleum ether (15 %) as eluents to obtain a yellow oily product. (b) Resultant product (1 equiv) from above step was dissolved in dry dichloromethane. A solution of 4 M HCl in dioxane (5:1 ratio w.r.t dichloromethane) was added dropwise at 0 °C to the reaction mixture and was allowed to stir for 3 h. The solvent was then evaporated under reduced pressure and product was precipitated out with diethyl ether to give compound **23.** Yield 95 %. ^{1}H-NMR (400 MHz, $CDCl_3$ + D_2O): *δ*: 0.61 (s, 3H), 0.89-1.96 (m, steroid), 2.22-2.44 (m, 2H), 3.76-3.97 (m, 2H), 4.76-4.81 (m, 1H), 5.07-5.14 (m, 2H), 7.29-7.38 (m, 5H).

General procedure for synthesis of amphiphiles (**A1-A20**).

Compound **23** (0.5 g, 1 equiv) was dissolved in dry dichloromethane. HOBt (1 equiv), DIPEA (1 equiv) and suitably protected amino acid (1.2 equiv) were added to the reaction solution and stirred at room temperature for 15 min. EDC.HCl (1.5 equiv) was then added to the reaction mixture portion-wise and the reaction was allowed to stir for 24-48 h at room temperature. We used following protected amino acids: Boc-Gly-OH, Boc-Ala-OH, Boc-Arg(pbf)-OH, Boc-Asn(Trt)-OH, Boc-Asp(OtBu)-OH, Boc-Gln(Trt)-OH, Boc-Glu(OtBu)-OH, Boc-His(Boc)-OH.DCHA, Boc-Ile-OH, Boc-Leu-OH, Boc-L-Lys(Boc)-OH.DCHA, Boc-Met-OH, Boc-Phe-OH, Boc-Pro-OH, Boc-Ser-OH, Boc-Thr-OH, Boc-Trp-OH, Boc-Tyr-OH, Boc-Cys(Trt)-OH, and Boc-Val-OH. Reaction mixture was diluted with dichloromethane (100 mL) and washed with saturated $NaHCO_3$ solution (2 x 100 mL) and brine solution (2 x 100 mL). The organic layer was separated and dried over anhydrous Na_2SO_4. Solvent was evaporated under reduced pressure and the crude products were purified by silica gel (230-400 mesh) column chromatography using ethyl acetate – petroleum ether.

Protecting groups in general, were deprotected using 4M HCl solution in dioxane except Boc-Asn(Trt)-OH, and Boc-Gln(Trt)-OH. For this, protected dipeptide-lithocholic acid conjugate (0.5 g, 1 equiv) was dissolved in dry dichloromethane (5 mL). A solution of 4M HCl in dioxane in 5:1 ratio (1 mL) was added dropwise to the reaction mixture. Reaction mixture was allowed to stir for 2 h

(12 h for Boc-Cys(Trt)-OH) at 0 °C and solvents were evaporated. Final products were precipitated with diethyl ether and was further dried under vacuum.

In the case of Boc-Asn(Trt)-OH and Boc-Gln(Trt)-OH, compound (0.5 g, 1 equiv) was dissolved in dry dichloromethane (5 mL). A solution of trifluoroacetic acid (2 mL) was added and reaction mixture was allowed to stir for 2 h at 0 ˚C. Solvents were evaporated, and final product was precipitated with diethyl ether and dried under vacuum. Trifluoroacetate salts were exchanged with Amberlite IRA 900 Cl resin to get the final molecules.

A1 (LCA-GE). ^{1}H-NMR (400 MHz, $CDCl_3$): δ: 0.63 (s, 3H), 0.91-1.96 (m, steroid), 2.27-2.42 (m, 3H), 2.71 (s, 2H), 3.92-4.12 (m, 2H), 4.52 (s, 1H), 4.77 (s, 1H), 5.09-5.15 (m, 2H), 7.28-7.37 (m, 5H), 8.02 (bs, 3H), 8.56 (bs, 1H). *HRMS (ESI/TOF) m/z: $[M + H]^+$ Calcd. for $C_{38}H_{57}N_2O_7^+$ 653.4160, Found 653.4.*

A2 (LCA-GD). ^{1}H-NMR (400 MHz, $CDCl_3$*): δ:* 0.61 (s, 3H), 0.89-2.04 (m, steroid), 2.19-2.39 (m, 2H), 2.65-2.59 (m, 2H), 3.93 (s, 2H), 4.49 (s, 1H), 4.73 (s, 1H), 5.06-5.13 (m, 2H), 7.34-7.54 (m, 5H), 8.59 (bs, 1H). *HRMS (ESI/TOF) m/z: $[M + H]^+$ Calcd. for $C_{37}H_{55}N_2O_7^+$ 639.4004; Found 639.4.*

A3 (LCA-GK). ^{1}H-NMR (400 MHz, CD_3OD): δ: 0.66 (s, 3H), 0.93-2.03 (m, steroid), 2.32-2.42 (m, 2H), 2.95-2.98 (m, 3H), 3.48-3.53 (m, 1H), 3.89-3.97 (m, 2H), 4.11 (d, 1H, *J* = 20 Hz), 4.73-4.80 (m, 1H), 5.12 (dd, 2H, *J* = 12 Hz, 6 Hz), 7.33-7.38 (m, 5H). HRMS (ESI): m/z $(C_{39}H_{61}N_3O_5)^+$ calcd, 651.4611; found, 652.4649 $(M)^+$*HRMS (ESI/TOF) m/z: $[M + H]^+$ Calcd. for $C_{39}H_{62}N_3O_5^+$ 652.4684, Found 652.4649.*

A4 (LCA-GR). ^{1}H-NMR (400 MHz, DMSO-d_6): δ: 0.58 (s, 3H), 0.81-1.97 (m, steroid), 2.22-2.38 (m, 2H), 2.43 (s, 1H), 3.12-3.15 (m, 2H), 3.75-4.05 (m, 3H), 4.60-4.70 (m, 1H), 5.03-5.11 (m, 2H), 7.32-7.37 (m, 5H), 7.78 (bs, 1H). *HRMS (ESI/TOF) m/z: $[M + H]^+$ Calcd. for $C_{39}H_{62}N_5O_5^+$ 680.4745, Found 680.4907.*

A5 (LCA-GH). ^{1}H-NMR (400 MHz, $CDCl_3$): δ: 0.61 (s, 3H), 0.88-2.39 (m, steroid), 3.06 (s, 1H), 3.33-3.47 (m, 2H), 3.96-4.13 (m, 2H), 4.56 (s, 1H), 4.76 (s, 1H), 5.07-5.14 (m, 2H), 7.29-7.35 (m,

5H), 8.47 (bs, 2H), 8.65 (bs, 1H), 8.92 (bs, 1H). *HRMS (ESI/TOF) m/z: [M + H]$^+$ Calcd. for $C_{39}H_{57}N_4O_5^+$ 661.4323, Found 661.4154.*

A6 (LCA-GQ). ^{1}H-NMR (400 MHz, DMSO-d_6+D_2O): δ: 0.54 (s, 3H), 0.83-1.95 (m, steroid), 2.09-2.15 (m, 1H), 2.25-2.32 (m, 3H), 3.84-4.05 (m, 2H), 4.61 (s, 1H), 5.00-5.08 (m, 2H), 7.16-7.32 (m, 6H). *HRMS (ESI/TOF) m/z: [M + H]$^+$ Calcd. for $C_{38}H_{58}N_3O_6^+$ 652.4320, Found 652.4479.*

A7 (LCA-GP). ^{1}H-NMR (400 MHz, $CDCl_3$): δ: 0.61 (s, 3H), 0.84-2.42 (m, steroid), 3.43-3.46 (m, 2H), 3.95 (q, 2H, *J* = 18Hz), 4.68-4.75 (m, 2H), 5.07-5.13 (m, 2H), 7.29-7.38 (m, 5H). *HRMS (ESI/TOF) m/z: [M + H]$^+$ Calcd. for $C_{38}H_{57}N_2O_5^+$ 621.4262, Found 621.4231.*

A8 (LCA-GN). ^{1}H-NMR (400 MHz, DMSO-d_6): δ: 0.56 (s, 3H), 0.83-1.89 (m, steroid), 2.25-2.38 (m, 2H), 2.54-2.68 (m, 2H), 3.82-3.93 (m, 2H), 4.06 (s, 12H), 4.63 (s, 1H), 5.02-5.09 (m, 2H), 7.15-7.34 (m, 6H). *HRMS (ESI/TOF) m/z: [M + H]$^+$ Calcd. for $C_{37}H_{56}N_3O_6^+$ 638.4164, Found 638.4320.*

A9 (LCA-GA). ^{1}H-NMR (400 MHz, $CDCl_3$+ D_2O): δ: 0.61 (s, 3H), 0.88-1.95 (m, steroid), 2.23-2.42 (m, 2H), 3.93 (q, 2H, *J* = 17 Hz), 4.17-4.22 (m, 1H), 4.71-4.76 (m, 1H), 5.06-5.13 (m, 2H), 7.29-7.37 (m, 5H). *HRMS (ESI/TOF) m/z: [M + H]$^+$ Calcd. for $C_{36}H_{55}N_2O_5^+$ 595.4105, Found 594.4033.*

A10 (LCA-GT). ^{1}H-NMR (400 MHz, DMSO-d_6): δ: 0.58 (s, 3H), 0.85-1.79 (m, steroid), 2.28-2.42 (m, 2H), 3.57-3.59 (m, 1H), 3.84-3.88 (m, 2H), 3.94-3.99 (m, 1H), 4.62-4.69 (m, 1H), 5.07 (dd, 2H, *J* = 8 Hz), 5.63 (s, 1H), 7.32-7.36 (m, 5H), 8.17 (bs, 3H), 8.93 (bs, 1H). *HRMS (ESI/TOF) m/z: [M + H]$^+$ Calcd. for $C_{37}H_{57}N_2O_6^+$ 625.4211, Found 625.4199.*

A11 (LCA-GS). ^{1}H-NMR (400 MHz, $CDCl_3$): δ: 0.61 (s, 3H), 0.89-1.93 (m, steroid), 2.20-2.39 (m, 2H), 2.65-2.95 (m, 2H), 3.93 (s, 1H), 4.49 (s, 1H), 4.73 (s, 1H), 5.06-5.12 (m, 2H), 7.34-7.54 (m, 5H), 8.59 (bs, 1H). *HRMS (ESI/TOF) m/z: [M + H]$^+$ Calcd. for $C_{36}H_{55}N_2O_6^+$ 611.4055, Found 611.4185.*

A12 (LCA-GV). ^{1}H-NMR (400 MHz, $CDCl_3$+ D_2O): δ: 0.61 (s, 3H), 0.89-1.96 (m, steroid), 2.17-2.49 (m, 2H), 3.91-4.06 (m, 3H), 4.69-4.75 (m, 1H), 5.10 (m, 2H), 7.29-7.37 (m, 5H). *HRMS (ESI/TOF) m/z: $[M + H]^+$ Calcd. for $C_{38}H_{59}N_2O_5^+$ 623.4418, Found 623.4539.*

A13 (LCA-GG). ^{1}H-NMR (400 MHz, $CDCl_3$): *δ*: 0.61 (s, 3H), 0.88-2.11 (m, steroid), 2.22-2.39 (m, 2H), 3.99 (s, 2H), 4.17 (s, 2H), 4.71-4.77 (m, 1H), 5.06-5.13 (m, 2H), 7.28-7.35 (m, 5H), 7.98 (bs, 3H), 8.56 (bs, 1H). *HRMS (ESI/TOF) m/z: $[M + H]^+$ Calcd. for $C_{35}H_{53}N_2O_5^+$ 581.3949, Found 581.3813.*

A14 (LCA-GM). ^{1}H-NMR (400 MHz, $CDCl_3$): δ: 0.61 (s, 3H), 0.89-1.96 (m, steroid), 2.10 (s, 3H), 2.24-2.30 (m, 2H), 2.36-2.44 (m, 1H), 2.66-2,68 (m, 2H), 3.94-4.06 (m, 2H), 4.43 (s, 1H), 4.77 (s, 1H), 5.07-5.14 (m, 2H), 7.30-7.35 (m, 5H), 8.29 (bs, 3H). *HRMS (ESI/TOF) m/z: $[M + H]^+$ Calcd. for $C_{38}H_{59}N_2O_5S^+$ 655.4139, Found 655.4299.*

A15 (LCA-GC). ^{1}H-NMR (400 MHz, $CDCl_3$): δ: 0.55 (s,3H), 0.86-1.88 (m, steroid), 2.26-2.37 (m, 2H), 2.70 (s, 1H), 3.00-3.08 (m, 2H), 3.88-3.96 (m, 2H), 4.09 (s, 1H), 4.67 (s, 1H), 5.07-5.09 (m, 2H), 7.34 (s, 6H), 8.45 (bs, 3H), 9.32 (s, 1H). *HRMS (ESI/TOF) m/z: $[M + H]^+$ Calcd. for $C_{36}H_{55}N_2O_5S^+$ 627.3826; Found 627.3808.*

A16 (LCA-GI). ^{1}H-NMR (400 MHz, $CDCl_3$): δ: 0.62 (s, 3H), 0.89-1.97 (m, steroid), 2.23-2.44 (m, 2H), 3.98 (s, 2H), 4.17 (s, 1H), 4.70-4.76 (m, 1H), 5.07-5.14 (m, 2H), 7.30-7.36 (m, 5H), 8.14 (bs, 3H). *HRMS (ESI/TOF) m/z: $[M + H]^+$ Calcd. for $C_{39}H_{61}N_2O_5^+$ 637.4575, Found 637.4728.*

A17 (LCA-GL). ^{1}H-NMR (400 MHz, $CDCl_3$): δ: 0.61 (s, 3H), 0.88-1.96 (m, steroid), 2.23-2.42 (m, 2H), 3.97 (s, 2H), 4.24 (s, 1H), 4.69-4.76 (m, 1H), 5.07-5.13 (m, 2H), 7.29-7.38 (m, 5H), 8.16 (bs, 3H), 8.39 (bs, 1H). *HRMS (ESI/TOF) m/z: $[M + H]^+$ Calcd. for $C_{39}H_{61}N_2O_5^+$ 637.4575, Found 637.4435.*

A18 (LCA-GY). ^{1}H-NMR (400 MHz, DMSO-d_6): δ: 0.56 (s, 3H), 0.84-1.90 (m, steroid), 3.05-3.16 (m, 1H), 3.84-3.97 (m, 3H), 4.64-4.70 (m, 1H), 5.04-5.11 (m, 2H), 6.70 (d, 2H, *J* = 8 Hz), 7.10 (d,

2H, *J* = 8 Hz), 7.30-7.39 (m, 5H), 8.15 (bs, 3H), 8.93 (bs, 1H), 9.41 (bs, 1H). *HRMS (ESI/TOF) m/z: [M + H]$^+$ Calcd. for $C_{42}H_{59}N_2O_6^+$ 687.4368, Found 687.4539.*

A19 (LCA-GF). ^{1}H-NMR (400 MHz, $CDCl_3$): δ: 0.61 (s, 3H), 0.81-1.95 (m, steroid), 2.23-2.44 (m, 2H), 3.96-4.02 (m, 1H), 4.44-4.47 (m, 1H), 4.60-4.65 (m, 1H), 7.22-7.56 (m, 10H), 7.94 (bs, 3H). *HRMS (ESI/TOF) m/z: [M + H]$^+$ Calcd. for $C_{42}H_{59}N_2O_5^+$ 671.4418, Found 671.4580.*

A20 (LCA-GW) ^{1}H-NMR (400 MHz, DMSO-d_6): δ: 0.54 (s, 3H), 0.83-1.83 (m, steroid), 2.23-2.30 (m, 1H), 2.35-2.42 (m, 1H), 3.06-3.17 (m, 1H), 3.27-3.37 (m, 1H), 3.85-4.13 (m, 4H), 4.66-4.71 (m, 1H), 5.08 (dd, 2H, *J* = 12 Hz, 5Hz), 7.01 (t, 1H, *J* = 8 Hz), 7.09 (t, 1H, *J* = 8 Hz), 7.25 (s, 1H), 7.31-7.7.39 (m, 6H), 7.71 (d, 1H, *J* = 8Hz), 8.12 (bs, 3H), 9.21 (bs, 1H). *HRMS (ESI/TOF) m/z: [M + H]$^+$ Calcd. for $C_{44}H_{60}N_3O_5^+$ 710.4527, Found 710.4382.*

8.3. Ethical statement. We used BALB/c or C57BL/6 mice (6-8 weeks old, female, weighing 18-20 g) or Sprague Dawley (SD) rats (6-8 weeks old, 180-200 g) for all the animal experiments carried out at either small animal facility of National Institute of Immunology New Delhi or Regional Centre for Biotechnology, Faridabad after due approvals (IAEC/AQ/2015/132, IAEC/AQ/2015/137, RCB/IAEC/2016/002, RCB/IAEC/2016/011) of the protocols by respective Institutional Animal Ethical Committees. We performed experiments with human blood samples after due ethical approval from the Institute Ethics Committee of Regional Centre for Biotechnology, Faridabad (RCB-IEC-H-7).

8.4. Gelation studies. We used an inverted vial assay for screening the amphiphiles for hydrogelation. Different amounts of amphiphile were taken in 1 mL of water (pH ~7.0) in a 5 mL glass vial. Suspensions were heated to boil and sonicated for complete dissolution of the amphiphile. The solution was allowed to cool and gelation was tested by inverting the vial and no flow under gravity implies the formation of gel.

8.5. Rheology studies. All the rheological experiments were performed using Rheoplus MCR102 (Anton-Paar, Graz, Austria) rheometer using a 25 mm cone-plate geometry with a cone angle being

1° at measuring the distance of 0.05 mm at 25 °C. A wet sponge is placed around the cone plate and base plate of the rheometer to act as a solvent trap. Hydrogels were carefully transferred over a plate and were subjected to amplitude sweep of 1 to 100 % strain at a constant frequency of 5 rad/s. Frequency sweep experiments were performed with a frequency range from 1 to 100 rad s^{-1} at 1 % strain.

8.6. Drug encapsulation and release studies. Drug encapsulation efficacy in A13 hydrogel was tested by taking different amounts of each drug (5, 10, 20 and 30 mg) along with A13 (70 mg) gelator in 1 mL of water (pH 7.4). The resultant suspension was heated to boil. The solution was allowed to cool at room temperature resulting in drug entrapped gel. For TRI-Gel formation, we used DOX (0.5 mg), CA4 (0.5 mg) and DEX (2.0 mg) in 1 mL of A13 gel (70 mg).

For drug release studies, TRI-Gel (1 mL) was taken in 5 mL flat bottom glass vial and incubated with PBS (pH 7.4 with 0.05 % Tween 80) (2 mL) at 37 ºC. At designated time points, PBS (1 mL) was collected and replaced by fresh PBS (1 mL). DOX release was quantified by UV absorption at 490 nm. For DEX and CA4 quantification, an aliquot of collected release media was evaporated to dryness and drugs were extracted using methanol (500 µL) twice by vortexing for 2 min followed by centrifugation. Supernatant methanol was completely dried. Final residue was reconstituted in methanol and transferred to HPLC vial. DEX and CA4 were quantified by Reverse phase-HPLC (Waters Ltd., Milford, USA) by injecting 10 µL of sample volume. Elution was carried out with isocratic solvent system (40 % acetonitrile and 60 % solvent mixture of water (37.5) : methanol (60) : tetrahydrofuran (2.5) with 0.2 % aq. NH_3) using TOSOH TSK-Gel ODS-100V 5 µm column (4.6 I.D. X 250 mm) (Waters Ltd., Milford, USA) with UV detection parameters for DEX at 238 and CA4 at 298 nm.

8.7. PBMC and RBC isolation. Blood was withdrawn from a healthy donor and centrifuged break free at 500 g for 15 min at room temperature in swinging bucket rotor. The supernatant was discarded and cell pellet was resuspended with 1X PBS in equal volume of plasma discarded.

Ficoll-hypaque was used for separating PBMCs and RBCs in separate layers and isolated by pipetting out from the tube one by one. First ficoll was layered in a 50 mL tube followed by slow addition of resuspended blood on top of it without disturbing the ficoll layer. Tube was centrifuged break free at 750 g for 15 min at room temperature in swinging bucket rotor. The middle whitish layer containing PBMCs was pipetted out and then whole supernatant was pipetted out leaving RBCs at bottom. The PBMCs and RBC's were given 2 washes separately with 1X PBS and used for hemolytic and live dead assay.

8.8. Hemolytic assay. Concentrated RBC solution (1 mL) was diluted in PBS (49 mL). RBCs (0.5 mL) solution was incubated with hydrogel (100 μL) and at different time points (1, 3 and 6h) supernatant was harvested and absorbance was measured at 541 nm. 1% Triton X-100 and PBS was taken as positive and negative controls respectively. Percentage of hemolysis was calculated as

Percent hemolysis = (Absorbance of the sample)-(Absorbance of negative control PBS)/ (Absorbance of positive control)-(Absorbance of negative control).

8.9. PBMC live dead assay. Isolated PBMCs were suspended in complete RPMI media with a concentration of 1 x 10^6 cells/mL. The 0.2 mL of PBMCs were incubated with 0.1 mL of hydrogel in 2 mL tubes for 1, 3 and 6 h. RPMI media and 0.2 mM Triton X-100 were taken as control. After incubation the cells were stained with propidium iodide (for dead cells) and Hoechst 33258 (for live cells) and analysed by BD FACS Verse (BD Biosciences, Franklin Lakes, New Jersey, USA).

8.10. Protein adsorption studies. The hydrogel was coated as a thin layer on a glass slide and incubated at 37 ^oC for 20 min for drying. The slide was then incubated with FITC-BSA (20 μg/mL in PBS) at 37^oC on mild shaking. Glass slides were removed at different time intervals, washed with PBS twice and visualized under fluorescence microscope. Polyethyleneimine (PEI) coated slides were used as a positive control. All the images were taken with auto exposure at 63X magnification using Nikon Eclipse Ti fluorescence microscope (Nikon Corp. Japan).

8.11. Gel degradation studies. A13 hydrogel (50 μL/well) in 12 well plate was incubated with and without esterase (100 U/mL) in PBS (2 mL) at 37 °C with shaking at 100 rpm. An aliquot (200 μL) of solution was taken out at different time intervals and absorbance at 600 was measured. For identification of degradation products, LC–MS and LC–MS/MS analysis of LCA-GG, LCA-OBn and LCA were performed on Linear Ion Trap Quadrupole (QTRAP 4500, SCIEX, USA) with Turbo VTM source and electrospray ionization (ESI) probe coupled to a high-pressure UHPLC (ExionLCTMAC, SCIEX, USA). Elution of each analyte was performed using Kinetex C-8 (50 x 2.1 mm), 1.7 μm (Phenomenex) column in positive ionization mode. 5 uL of the sample was injected through autosampler into UPLC flow and LC analysis was performed. Enhanced Product Ion (EPI) scan and Multiple Reaction Monitoring (MRM) were used for identification of ester cleaved product ion of LCA-GG. Q1 precursor ion and Q3 product ion (Q1/Q3 transition) of LCA-GG, LCA-OBn and LCA are 581.400/581.400, 485.500/467.300 and 359.300/341.400 m/z respectively during MRM scan. Data acquisition and processing were carried out using Analyst 1.6.3 and MultiQuant 3.0.2 (SCIEX, USA) software.

8.12. Biocompatibility studies in animal models. Animals (BALB/c mice) were shaved at the flank region to remove hair before the start of an experiment. A13 gel (7 %) was subcutaneously injected at the flank region of animals. BALB/c mice were sacrificed on different days to observe the injected gel and to collect the gel-tissue interface for histochemical and CD45 staining.

For H&E staining, gel-tissues were isolated, soaked in 4 % paraformaldehyde solution for 24 h and preserved in cryomatrix at -80 °C. The frozen tumor samples were subjected to cryo-sectioning using cryotome (Microm HM550, Thermo Scientific) to get 6-8 μm thin sections. Tissue sections were taken on poly-lysine coated glass slides and stored at -80 °C. For staining, sections were thawed at room temperature and fixed with 4 % paraformaldehyde for 5 min followed by PBS wash. Tissue sections were dried and dipped in hematoxylin solution for 1 min followed by rinsing with MiliQ water for 1-2 min to remove extra strain. Sections were then dipped in lithium carbonate

solution (1.5 % w/v), a bluing agent, for 1 min followed by a wash in 70 % ethanol. The slides were then dipped in eosin solution for 3 min and washed with MiliQ water twice. Then slides were rinsed with the gradient of alcohol (70, 80 and 100 %) followed by two washes in xylene for 10 min each. The slides were dried, mounted with DPX mount and kept for 24 h to solidify the DPX and images were taken on Olympus BX43 microscope with D.P. 26 camera at 10X and 40X magnification in stitching mode to get a larger section of skin along with gel.

8.13. *In vivo* fluorescence probe release studies. Near-infrared (NIR) dye, IR820, (100 μg) entrapped A13 gel (7 %) (200 μL) was injected subcutaneously in BALB/c mice (n = 3) or SD rats (n = 3). In another set of mice (n = 3) or rats (n = 3), subcutaneous injection of an aqueous solution of NIR dye (without A13 gel) was injected. Whole body fluorescence imaging at different time points was performed using SPECTRUM In Vivo Imaging System (IVIS) (PerkinElmer, Santa Clara, CA, USA) by setting an excitation filter at 710 nm and an emission filter at 820 nm with an exposure time of 5 sec. Animals were anesthetized using 1.5 % isoflurane in the chamber and transferred to IVIS under isoflurane for imaging.

8.14. Anticancer activities. All anticancer studies were performed using syngeneic Lewis lung carcinoma (LLC) model in C57BL/6 mice unless specified. LLC cells were cultured in DMEM media supplemented with 10 % FBS and 1X antibiotic solution at 37 ^{o}C with 5 % CO_2.

Optimization of DOX entrapped A13 gel. The flank region of mice were shaved to remove hair before the start of the experiment. On day 0, LLC cells (1.5×10^6) suspended in FBS : Matrigel (1:1, 200 μL/mouse) were injected subcutaneously in the flank region of mice. On day 3, when tumors reach ~30-40 mm^3, mice were randomized into different groups (n = 7/group) and were subjected to different treatments. Group 1 mice were left untreated. Group 2-5 mice were treated with subcutaneous injection of different doses of DOX (2.5, 5, 10 and 25 mg/kg of mice bodyweight) entrapped in A13 gel (200 μL/mouse) near the tumor site (< ~1 cm). Tumor volume and bodyweight

of mice were measured on alternate days. Tumor volume was calculated using formula L x $B^2/2$ where L is length and B is breadth of the tumor. Mice (n = 6) were observed for survival.

Optimization of CA4 entrapped A13 gel. The protocol is same as described in above where different doses of CA4 (5, 10, 25 and 50 mg/kg of mice body weight) entrapped in A13 gel (200 μL/mouse) were used.

Effect of TRI-Gel therapy. In this experiment, LLC tumor-bearing mice were randomized into four different groups (n = 7 mice/group) and subjected to different treatments on day 3. Group 1 mice were left untreated. In group 2 (represented as TRI-TS), mice were treated with subcutaneous injection of a combination of DOX (5 mg/kg), CA4 (5 mg/kg) and DEX (20 mg/kg) suspension (using 5 % polysorbate 80 (TWEEN 80) and 2.5 % DMSO) in saline near tumor site without hydrogel. Group 3 (represented as TRI-Gel), mice were treated with subcutaneous injection of a combination of DOX (5 mg/kg), CA4 (5 mg/kg) and DEX (20 mg/kg) entrapped in A13 gel (200 μL/mouse) near the tumor site (< ~1 cm). In group 4 (represented as TRI-IV), mice were treated with intravenous injection of DOX (0.5 mg/kg) and CA4 (0.5 mg/kg) in saline, and oral delivery of DEX (2 mg/kg) in carboxymethylcellulose (0.5 %) and Tween 80 (4 %) mixture on alternate day for 20 days (total 10 doses). Tumor volume and body weight of mice was measured on alternate days. For lipidomics, RNA sequencing and validation studies, mice were sacrificed on day 21. Tumors were isolated and stored in Allprotect tissue reagent at -80 °C. Similar protocol and conditions were used to test the efficacy of TRI-Gel treatment in murine breast cancer (4T1) model.

Effect of dual and triple drug combinations. In this experiment, LLC tumor-bearing mice were randomized into five different groups (n ≥ 6/group) and subjected to the following treatments. Group 1 mice were left untreated. Mice in group 2, 3 and 4 were treated with subcutaneous injection of combination of two drugs entrapped in A13 gel (200 μL/mouse) like in group 2 mice (represented as DOX-DEX-Gel) combination of DOX (5 mg/kg) and DEX (20 mg/kg), in group 3 mice (represented as DOX-CA4-Gel) combination of DOX (5 mg/kg) and CA4 (5 mg/kg) and in group 4

(represented as DEX-CA4-Gel) combination of DEX (20 mg/kg) and CA4 (5 mg/kg) was used. Mice in group 5 were treated with TRI-Gel therapy. Tumor volume of mice was measured on alternate days.

Effect of *Gba1* knockdown on TRI-Gel therapy. LLC tumor-bearing mice were randomized and subjected to the following treatments (n ≥ 5/group). Group 1 mice were left untreated. In group 2, mice were treated with TRI-Gel therapy. Group 3 and 4 mice were treated with an intra-tumoral injection of siRNA-polymer complexes (50 μL/mouse) in an interval of every two days (Day 2, 5, 8, 11 and 14) and with TRI-Gel therapy on day 3. In group 3, *Gba1* siRNA was used and in group 4, *scrambled* siRNA was used. Group 5 mice were treated with only *Gba1* siRNA. Tumor volume and body weight of mice were measured on alternate days. On day 21, mice (n = 6) were sacrificed, tumors were isolated and stored in Allprotect tissue reagent at -80°C for further validations.

For siRNA-polymer complexes, *Gba1* or *scrambled* siRNA (10 µL of 20 µM) was mixed with a cationic polymer (TAC6) (100 µL, 1 mg/mL) and incubated for 20 min at room temperature.[1] Sodium aspartate (10 µL, 1 mg/mL) was then added to it, mixed by pipetting and incubated. After 10 min, siRNA-polymer complexes were diluted with PBS to make a final volume of 600 µL. Each mouse was given a dose of 200 ng siRNA (50 µL of siRNA complexes) and a total of five doses were used.

8.15. Tumor single-cell profiling. Freshly isolated tumors were chopped into small pieces and kept for digestion in a 3-4 mL mixture of collagenase IV (0.7 mg/mL) and DNAse I (50 U/mL) in HBSS (Hank's balanced salt solution) for 45 min at 37ºC with constant shaking. The digestion was stopped by addition of complete RPMI media. Single cells were strained through 40 µm cell strainer and pelleted down. Any RBC contamination was removed by ACK buffer mediated RBC lysis. The cells were then re-suspended in 1X PBS and counted using haemocytometer. Approximately $1*10^6$ cells were taken into 1.5 mL tube and stained with CD31-PE (1:500) and CD45-APC-Cy7 (1:500) antibodies in staining buffer for 20 min in dark at room temperature. Cells were then washed twice

with PBS and acquired on BD FACS Canto II (BD Biosciences, BD Biosciences, Franklin Lakes, New Jersey, USA).

For Ki67 intracellular staining, single cell suspension containing 1 x 10^6 cells was washed twice with PBS. 3 mL of 70% ethanol was then added drop by drop to the pellet with continuous vortexing. The suspended cells were then incubated at -20 °C for 2 h to complete the permeabilization step. The permeabilized cells were then washed twice with PBS and stained with Ki67-PerCp-Cy5.5 (1:500) at room temperature for 30 min in dark. The cells were then washed twice with PBS. Cells were finally suspended in 200 µL of PBS and acquired on BD FACS Canto II (BD Biosciences, BD Biosciences, Franklin Lakes, New Jersey, USA).

For apoptosis assay, single cell suspension containing 1 x 10^6 cells were stained with PI (1 µg/mL) and Annexin V-FITC (1:200) in presence of freshly prepared annexin binding buffer and incubated at room temperature for 30 min in dark. The cells were then washed twice with PBS. Cells were finally suspended in 200 µL of PBS and acquired on BD FACS Canto II (BD Biosciences, BD Biosciences, Franklin Lakes, New Jersey, USA).

8.16. TUNEL assay and Immunofluorescence studies. For TUNEL assay, terminal deoxynucleotidyl transferase (TdT) dUTP Nick-End Labeling assay was performed. The frozen tissue sections were thawed at room temperature and fixed with 4 % paraformaldehyde for 5 min followed by PBS wash. Permeabilization of tissue was performed by boiling the slides in 0.1 M citrate buffer in a microwave for 1 min followed by quick transfer to MiliQ water at room temperature. Slides were dipped in 1x PBS twice and dried using tissue paper. The labeling reaction was set up by adding 50 µL of TUNEL reaction mixture on the tissue section. Sections were covered with parafilm and incubated at 37 °C for 2 h in a humidified chamber. Labeling mixture without enzyme was used as negative control. Slides were then rinsed with 1X PBS thrice. The sections were counterstained with Hoechst 33258 (1:10000 dilution from 5 mg/ml stock) for 30 seconds followed

by PBS wash. The sections were mounted with Prolong gold and kept in the dark at room temperature to dry.

For immunofluorescence studies, tissue sections were fixed with 4 % paraformaldehyde for 5 min followed by PBS wash. Antigen retrieval of tissue sections was performed in citrate buffer (pH 6.0) for 10 min at 121 °C followed by PBS wash. Sections were then incubated in blocking buffer (5 % goat serum in PBS) for 30 min at room temperature followed by incubation with primary antibodies Ki67 in 1:1000 dilution, CD45 in 1:800 dilution, *α*-SMA in 1:300 dilution, P-gp in 1:300 dilution, Gba1 in 1:300 dilution for overnight at 4°C. Sections were then washed two times with PBST (PBS with 0.05 % Tween 20) and incubated with anti-mouse or anti-rabbit conjugated with Alexa fluorophore 594 (1:800 dilution) antibody for 2 h at room temperature. Sections were washed with PBST and then counterstained with Hoechst 33258 (1:5000 dilution) for 1 min followed by PBS wash. Sections were mounted with Prolong gold and kept in the dark at room temperature for overnight.

Confocal imaging of the samples was performed with Leica TCS SP5 or SP8 or Zeiss LSM880 confocal microscope. Sections were visualized at 40X oil immersion using LAS AF and ZEN 2.3 SP1 FP1 software. Z-stacking was performed and images were acquired for each section. Images were processed using LAS X software. The processed images were quantified using ImageJ software (NIH). Individual blue and red channel were separately quantified. The images were converted to 8-bit type followed by adjusting the threshold for signal quantification. Signals were counted for each channel and presented as (Red signal/Blue signal) * 100 that is a number of positive signals per field. At least three tissue sections per tissue sample and three tissue samples for each treatment were used for quantification.

8.17. Lipid extraction. Tumors tissues (~50 mg) were homogenized by ceramic beads in 2 mL homogenizing tubes (Precellys homogenizer, Bertin Technologies, France) in PBS (200 μL). An aliquot (20 μL) was taken for protein estimation by bicinchoninic acid (BCA) protein estimation kit.

1 mg protein equivalent of each sample was used for lipid isolation using a previously published protocol with some modifications.[2] Tissue suspensions were transferred to Teflon-lined borosilicate tubes. Chloroform ($CHCl_3$): Methanol (MeOH) (1:2) (3 mL) and LIPID MAPS™ internal standard (IS) cocktail Sphingolipid Mix II (5 μL of 25 μM/ 125 pmol of each lipid species) was added to the suspension. Sphingolipid Mix II is a mixture of C17-sphingosine, C17-sphinganine, C17-sphingosine-1-phosphate, C17-sphinganine-1-phosphate, C12-ceramide, C12-ceramide-1-phosphate, C12-sphingomyelin, C12-glucosylceramide and C12-lactosylceramide. Samples were sonicated (3 x 20 sec on and 30 sec off-cycle, amplitude 30, Sonics Vibra Cell VCX130, USA) and single-phase mixture was incubated at 48 °C for overnight in a water bath. After cooling, 75 μL of 1 M potassium hydroxide (KOH) dissolved in MeOH was added, sonicated briefly and incubated in a shaking water bath for 2 h at 37 °C. After cooling, samples were neutralized using glacial acetic acid (3-5 μL). One aliquot (1.5 mL) was centrifuged to remove the debris and supernatant was used as single-phase (SP) extract for estimation of sphingolipids. Other aliquot (organic phase/OP) was then diluted with $CHCl_3$ (1 mL) and water (3.5 mL), vortexed, centrifuged and lower layer (OP) transferred to new tube. The upper part was re-extracted two more times with $CHCl_3$ (1 mL) and lower layer was transferred to the same tube.

The solvents were evaporated using N_2 gas source and the dried sample was reconstituted in 300 μL of mobile phase solvent that is a mixture of solvent A and solvent B in 20:80 ratio. SP sphingolipids were resuspended and separated using solvent A and solvent B where solvent A is mixture of CH_3OH, water and HCOOH in 58:41:1 ratio and solvent B is a mixture of CH_3OH and HCOOH in 99:1 ratio both with 0.5 mM ammonium formate. OP sphingolipids were separated in solvent A and solvent B where solvent A is mixture of water and HCOOH in 99.8:0.2 ratio and solvent B is mixture of CH_3OH and HCOOH in 99.8:0.2 ratio, both with 5 mM ammonium formate. The resulting OP and SP extracts for each sample were sonicated for 15 sec, vortexed and centrifuged at 13000 rpm for 5 min. The clear supernatant was transferred to the autoinjector vial

for LC-MS/MS analysis (ceramide-1-phosphate and sphingosine-1-phosphate from SP extracts and ceramide, glucosylceramide and lactosylceramides from OP extracts).

8.18. LC-MS/MS method and data analysis. Sphingolipids were analyzed by reverse-phase ultra-high-pressure liquid chromatography (Prominence XR UHPLC, Shimadzu, USA) using an Acquity BEH C18, 2.1 × 50 mm column (Waters Ltd., Milford, USA) with a particle size of 1.7 µm kept at 60 °C, coupled to a hybrid triple quadrupole/linear ion trap mass spectrometer (4500 Q TRAP, SCIEX, USA). Total run time was optimized for 16 min for OP samples and 8 min for SP samples where solvent A and solvent B were used as mobile phase A and B respectively with a total flow rate of 0.3 mL/min. Elution conditions were followed as per standardized methods with certain modifications.[2,3] Sphingolipids were monitored using Scheduled Multiple Reaction Monitoring (MRM) with preidentified retention time. Scheduled MRM experiment was performed in positive ionization mode, where Q1 (precursor ion mass) and Q3 (product ion mass) for all transitions and compound dependent parameters like Declustering Potential (DP), Entrance Potential (EP), Collision Cell Exit Potential (CXP) and Collision Energy (CE) were optimized as per details provided.[2,3] An MRM to Enhanced Product Ion (EPI) scan was used. Source dependent parameters like nebulizer gases GS1 (50 psi), GS2 (50 psi), curtain gas (25 psi), temperature (600 ^{o}C) and ion spray voltage (5.5 KV) were optimized.

Standard curve was generated for absolute quantitation of sphingolipids. The linearity of the calibration curve was ascertained for C16:0-ceramide, C16:0-ceramide-1-phosphate, C16:0-lactosylceramide and C18:1-sphingosine-1-phosphate (0.78 to 200 pmol) and C16:0-glucosylceramide (3.9 to 500 pmol) using the corresponding commercially available natural standards. Each standard was serially diluted in A + B solvent mixture and 10 µL injection volume was used. Linear regression lines were plotted with correlation coefficient values of at least 0.99. To quantify absolute value of sphingolipids in tumor samples, the extracted ion chromatograms were examined. The area under the peaks for both analytes and spiked

sphingolipid internal standard were estimated and ratio of each analyte with respective internal standard (C12:0-ceramide, C12:0-glucosylceramide, C12:0-lactosylceramide, C12:0-ceramide-1-phosphate and C17:1-sphingosine-1-phosphates) were determined. These ratio values were used to quantitate the sphingolipids in tumor samples equivalent to 1 mg protein. Four independent biological replicates (n = 4) were used and for each sample, three technical replicates were run with three blank runs between each sample. All statistical analyses were performed by two-tailed unpaired *t*-test analysis using GraphPad Prism version 7.0 (GraphPad Software, La Jolla, CA, USA).

8.19. RNA isolation and RNA sequencing analysis. Frozen tissues in Allprotect Tissue Reagent were homogenized in Trizol. RNA was purified by Phenol:Chloroform:Isoamyl alcohol extraction followed by ethanol precipitation. The RNA concentration was determined using NanoDrop 2000 (Thermo Scientific, USA). The integrity and quality of ribosomal 28S and 18S were determined on the agarose gel. Any traces of genomic DNA were removed by DNase1 treatment for 30 min at 37 ^{o}C followed by heat inactivation using 50 mM EDTA. Quality control of RNA was done using Bioanalyzer 2100 RNA 6000 NanoAssay chip (Agilent Technologies, Santa Clara, USA) and RNA with RIN > 8 was included for the study. The cDNA libraries were constructed by TruSeq RNA Library Prep Kit v2 (Illumina Inc., USA). Sequencing (100 bp paired-end) was performed using Illumina Hi Seq2500 (Macrogen Inc. Korea).

Imaging, base calling and quality scoring were done as per standard manufacturer's guidelines (Illumina Inc., USA). The sequence quality was checked with FastQC and adapter trimming was done with Trimmomatic. Reads were aligned with STAR aligner against mouse reference genome [Genome Reference Consortium Mouse Build 38 (GCA_000001635.2)]. Transcriptome assembly and read counting were performed using String Tie and differential expression analysis was done using Ballgown. A fold change ± 1.5 and *p*-value ≤ 0.05 (Fisher's Exact test) were used to filter differentially expressed genes. GO-term enrichment analysis was performed using the Database

for Annotation, Visualization and Integrated Discovery (DAVID). All the RNA sequencing data has been submitted to NCBI as mentioned in supporting information.

8.20. Alternative Splicing (AS) analysis. Differential alternative splicing (AS) in untreated, DOX-Gel, DEX-Gel, CA4-Gel and TRI-Gel treated tumor samples (included in triplicate) were identified by Exon Pointer (EP) and Intron Pointer (IP) algorithm as per published protocol.[4] TopHat2 pipeline was used to extract the information of junction reads. Raw read counts for exons and introns were then obtained using R subread package from output BAM files of TopHat2 aligner. The read counts for exons, introns and junctions were subjected to TMM normalization implemented in edge R package and later converted to expression using Limma voom function. Two matrices; Design matrix –describing experiment and contrast matrix – to perform the desired statistical test were provided to Limma. EP and IP combine the information inbuilt in exon, intron, flanking junction and skipping junction to pinpoint an exon/intron as alternatively spliced. For example, to detect cassette exons (CE), the reads mapped to the CEs, its flanking junctions and the skipping junction that results from the exclusion of the CE were combined together. EP works on the logic that if the exon is included then exon and its flanking junction should be expressed while skipping junction should not be expressed and vice-versa. For intron retention (IR), only reads that mapped to intron and their skipping junction are utilized with the condition that if intron is included in transcript then skipping junction should not be expressed and vice-versa.

8.21. GO enrichment analysis. Enrichment analysis of all differentially expressed genes and genes predicted by AS analysis for cassette exon (CE) and intron retention (IR) events were performed using DAVID. All default parameters were used and cut off was kept at p-value ≤ 0.05 (Fisher's Exact test) and/or false discovery rate (FDR) of ≤ 25.0. The functional association was done using Biological processes (GO_BP_Direct) and KEGG Pathways. The raw data and values are provided in **Data sets S3, S7 and S8**.

For ontology analysis of significantly altered genes in response to DOX-Gel, DEX-Gel, CA4-Gel and TRI-Gel treatments (Pie chart representation as shown in Figure S11D), all upregulated and downregulated genes for each treatment were subjected to ontology analysis with R package topGO. We used all the genes in the array as the background. Ontology terms showing *p* values ≤ 0.05 by Fisher's exact test (weight algorithm) were considered for further analysis. Followed by curation, the terms were manually categorized into nine key biological processes. The raw data and values are provided in the **Data set S4**.

8.22. Quantitative Real-Time PCR. For quantitative Real-Time PCR (qRT-PCR), cDNA was synthesized using 1 μg RNA by iScript cDNA synthesis kit. Gene expression analysis was done by quantitative Real-Time PCR (qRT-PCR) using iTaq Universal SYBR Green Supermix on Ariamax Real-Time PCR system (Agilent Technologies, USA). Relative quantitation of gene expression was done using β-actin as the endogenous reference gene for normalization. All primers sequences used for qRT-PCR are listed in **Table S2**.

Semi-quantitative PCR to validate isoform-specific AS events was done for 36-40 cycles using Taq polymerase. PCR products were resolved on 2 % agarose gel along with 100 bp ladder. *Gba1* intron retained bands were quantified using ImageJ software (NIH) and divided with the intensity of the β-actin band. All primers sequences used for semi-quantitative PCR are listed in **Table S3**. Original gel pictures are shown in **Data Figure ES7** and **Data Figure ES8A**.

8.23. Western Blot. Tumor tissues were homogenized in RIPA lysis buffer with 1 mM phenylmethanesulfonyl fluoride for 1 min using hand homogenizer (Polytron PT-MR 166 E, Kinematica AG, Switzerland) and kept on ice for 2 min. This cycle was repeated five times and samples were placed on ice for 10 min and vortexed for 15 sec. Tissue debris was removed by centrifugation and supernatant was collected. Protein concentration was determined by bicinchoninic acid (BCA) protein estimation kit. Protein samples (35 μg) were denatured, run on 10 % SDS-polyacrylamide gel and transferred on to nitrocellulose membrane. Membranes were

blocked with 5 % BSA dissolved in 1X TBST (TBS with 0.1 % Tween 20) for 1 h. Primary antibodies used were rabbit polyclonal Gba1 (1:500 dilution in 5 % BSA in TBST for overnight at 4 ^{o}C) and β-actin (1:5000 dilution in 5 % BSA in TBST for overnight at 4^{o}C). After incubation with primary antibody, membranes were washed thrice with 1X TBST and incubated with secondary antibody anti-rabbit conjugated to HRP (1:10000 for Gba1) and anti-mouse conjugated to HRP (1:5000 for β-actin) for 1 h at room temperature. Blots were washed 4-5 times with 1X TBST for 10 min and developed using an enhanced chemiluminescent substrate. Original immunoblot picture is shown in **Data Figure ES8B**.

8.24. Enzymatic assay for GBA1 activity.[5] Tumor tissues were homogenized in homogenization buffer of sodium taurocholate (0.25 %), Triton X-100 (0.25 %) and citrate-phosphate buffer (150 mM). Homogenized solution was subjected to two freeze-thaw cycles (-80 ^{o}C to 4 ^{o}C) followed by incubation in ice for 30 min. The homogenized solution was centrifuged at 20,000x g for 20 min and the supernatant was collected for activity assay. Protein concentration was determined using BCA protein assay kit. Protein (50 μg) from each sample was mixed with 60 μg of 4-methylumbelliferyl β-glucopyranoside substrate (Stock solution: 1 mM in 1 % BSA) in homogenization buffer (200 μL). The solution was incubated at 37 °C in the dark for 30 min and the reaction was stopped by addition of 1M glycine (pH 12.5) (200 μL). Fluorescence of product, 4-methylumbelliferone, was measured in a 96-well plate (clear/black bottom) using SpectraMax M5 multimode microplate reader (Molecular Devices, Sunnyvale, CA, USA) with λ_{ex} of 355 nm and λ_{em} of 460 nm. Amount of product formed was calculated by a standard curve generated from the fluorescence of 4-methylumbelliferone. Gba1 activity is represented in terms of the percentage of the amount of product formed for each sample as compared to control samples.

8.25. Statistical analysis. We used two-tailed Student's *t*-test to compare differences between two experimental groups and two-way ANOVA with Tukey post hoc test for comparing time-dependent experiments with multiple groups. Log-rank Mantel-Cox test was used in analysis of survival

experiments. $P < 0.05$ was considered as a statistically significant difference. Statistical analysis was performed using Prism 7 (GraphPad Software).

9. Deposited Data

Raw Sequencing Data	This paper	All the RNA-seq data related to this study have been deposited in SRA with the accession codes: SRR7897085, SRR7897086, SRR7897084, SRR7897087, SRR7897089, SRR7897088, SRR7897090, SRR7897091, SRR7897082, SRR7897083, SRR7897077, SRR7897080, SRR7897081, SRR7897078, SRR7897079 at following links: https://www.ncbi.nlm.nih.gov/sra/?term=SRR7897085 https://www.ncbi.nlm.nih.gov/sra/?term=SRR7897086 https://www.ncbi.nlm.nih.gov/sra/?term=SRR7897084 https://www.ncbi.nlm.nih.gov/sra/?term=SRR7897087 https://www.ncbi.nlm.nih.gov/sra/?term=SRR7897089 https://www.ncbi.nlm.nih.gov/sra/?term=SRR7897088 https://www.ncbi.nlm.nih.gov/sra/?term=SRR7897090 https://www.ncbi.nlm.nih.gov/sra/?term=SRR7897091 https://www.ncbi.nlm.nih.gov/sra/?term=SRR7897082 https://www.ncbi.nlm.nih.gov/sra/?term=SRR7897083 https://www.ncbi.nlm.nih.gov/sra/?term=SRR7897077 https://www.ncbi.nlm.nih.gov/sra/?term=SRR7897080 https://www.ncbi.nlm.nih.gov/sra/?term=SRR7897081 https://www.ncbi.nlm.nih.gov/sra/?term=SRR7897078 https://www.ncbi.nlm.nih.gov/sra/?term=SRR7897079

10. References

1. Yavvari, P. S.; Verma, P.; Mustfa, S. A.; Pal, S.; Kumar, S.; Awasthi, A. K.; Ahuja, V.; Srikanth, C. V.; Srivastava, A.; Bajaj, A. A nanogel based oral gene delivery system targeting SUMOylation machinery to combat gut inflammation. *Nanoscale* **2019**, *11*, 4970–4986.
2. Shaner, R. L.; Allegood, J. C.; Park, H.; Wang, E.; Kelly, S.; Haynes, C. A.; Sullards, M. C.; Merrill, A. H. J. Quantitative analysis of sphingolipids for lipidomics using triple quadrupole and quadrupole linear ion trap mass spectrometers. *J. Lipid Res.* **2009**, *50*, 1692–1707.
3. Dasgupta, U.; Bamba, T.; Chiantia, S.; Karim, P.; Tayoun, A. N. A.; Yonamine, I.; Rawat, S. S.; Rao, R. P.; Nagashima, K.; Fukusaki, E.; Puri, V.; Dolph, P. J.; Schwille, P.; Acharya, J. K.; Acharya, U. Ceramide kinase regulates phospholipase C and phosphatidylinositol 4, 5, bisphosphate in phototransduction. *Proc. Natl. Acad. Sci. U. S. A.* **2009**, *106*, 20063–20068
4. Tabrez, S. S.; Sharma, R. D.; Jain, V.; Siddiqui, A. A.; Mukhopadhyay, A. Differential alternative splicing coupled to nonsense-mediated decay of mRNA ensures dietary restriction-induced longevity. *Nat. Commun.* **2017**, *8*, 306.
5. Marshall, J.; McEachern, K. A.; Kyros, J. A. C.; Nietupski, J. B.; Budzinski, T. L.; Ziegler, R. J.; Yew, N. S.; Sullivan, J.; Scaria, A.; van Rooijen, N.; Barranger, J. A.; Cheng, S. H. Demonstration of feasibility of in vivo gene therapy for gaucher disease using a chemically induced mouse model. *Mol. Ther.* **2002**, *6*, 179–189.